Computational Investigation of Covalent Organic Pyrgos[n]cages as Potential Dual Modulators of VEGFR-2 D2-D3 domain and DNA Structural Interfaces

Biswajit Mohanty, Parthapratim Munshi*
Multifunctional Molecular Materials Laboratory, Department of Chemistry,
School of Natural Sciences, Shiv Nadar Institution of Eminence Deemed to be University,
Delhi-NCR, Uttar Pradesh-201314, India
*Correspondence: parthapratim.munshi@snu.edu.in

Computational Methodologies

1. DFT analysis of PC[n] and nucleobase complexes

PC[n]s are π-stacked supramolecular architectures composed of axially fused imidazolium units forming the vertical walls, while phenyl rings act as the top and bottom caps of the macrocyclic framework. The structures of the PC[2] were extracted from the crystal lattice and optimized using various dispersion D3[1] corrected DFT-functional with def2TZVPP level of theory to alleviate the self-interaction error[2] (SIE), which is significant in cationic systems, where the loss of an electron can amplify the spurious interactions. Normal mode analysis ensures the absence of imaginary frequencies in the optimized structure, thereby revealing the global minimum, which is then compared to its crystal structure. The DFT functional includes global hybrid (GH) generalized gradient approximation (GGA) (B3LYP, PBE0, B3PW91), local GGA (BLYP, B97, PBE, BP86, BPBE), GH meta GGA (M05, M06, M052X, M062X), Local meta GGA (TPSS), range separated hybrid (RSH) GGA (CAM-B3LYP, LC-ωPBE).[3–7] B3PW91-D3/def2TZVPP is regarded as a suitable functional that achieves a near approximated crystal geometry with cost-effective computations. Further, we optimized the monomer PC[1] derived from the PC[2] crystal structure and extensively studied it in complex with nucleobases to deepen our understanding of PC[n] and DNA binding. The binding energy and zero-point energy (ZPE) were computed to determine the structure and stability of the PC[1]-nucleobase complex. The basis-set superposition error (BSSE)-corrected binding energy for each complex was analysed using the supermolecular approach and subsequently subjected to the counterpoise correction proposed by Boys and Bernardi. [8]

2. Structural analysis of VEGF-A/C/E@VEGFR-2D23

The VEGFR-2 and D2-D3 regions represent immunoglobulin (Ig) homology domains organized into two antiparallel β-sheets. Domain D2 adopts a compact, globular fold with relatively short β-strands, whereas D3 forms a more elongated architecture characterized by extended β-strands in both sheets. Both domains share a conserved intradomain disulfide bond linking the opposing β-sheets, which is buried within the hydrophobic core and contributes to structural stability. The overall arrangement of D2 and D3 is extended, with the two domains separated by a short Val-Gly-Tyr tripeptide linker that permits minimal interdomain contacts, thereby favoring a relatively independent structural organization of each module. Brozzo[9,10] et al. and Leppänen et al. investigated the crystal structures (Figure S2) and binding affinities of VEGF-A (3V2A), VEGF-C (2X1X), and VEGF-E (3V6B) to VEGFR-2D23. To determine the participating residues involved in the VEGFR-2D23/VEGF-A/C/E docking, we analyzed their interactions using PPI3D, a web server for searching, analyzing, and modeling protein interactions in the context of 3D structures.[11] It is interesting to observe that VEGF-A binds exactly between the D2 and D3, while VEGF-C is preferred to bind the D2 domain, and VEGF-E is biased to D2 with negligible interaction with D3.

3. MD simulation of PC[n]s with VEGFR-2D23 and DNA

The PC[n]s (n = 1-4) were docked using AutoDock Vina-1.1.2[12] with the VEGFR-2D23 and DNAs (duplex DNA and 3WJ). Docking studies indicate the potential of these cationic ligands to bind to VEGFR-2D23 and DNA. All-atom MD simulations using Amber 23[13] were employed to investigate the conformational stability and binding dynamics of the VEGFR-2 extracellular domains D23 in complex with the PC[n]s ligand (n = 1-4). The initial VEGFR-2 structure and the DNAs were extracted from the RCSB database for VEGFR-2 (PDB ID: 3V2A[9]), duplex DNA (PDB ID: 4U8A[14], 5'-CGCGAATTCGCG-3'), and the 3WJ DNA (PDB ID: 3I1D[15], 5'-CGTACG-3'). The PC[n] were parametrized using restrained electrostatic potential[16] (RESP) charges derived from quantum chemical calculations at the B3LYP/6-31+G(d) level with a SMD implicit water solvation model and the Merz-Kollman scheme using the Gaussian16[17] program. VEGFR-2D23 parameters were taken from the AMBER ff14SB force field[18], while the DNAs are parameterized using the OL15 force field[19], and ligand topologies were generated using GAFF2. All systems were explicitly solvated in a rectangular TIP3P water box extending 15 Å from the solute, and neutralized with counterions (Cl^-, for VEGFR-2D23, and Na^+ for DNAs) to ensure electrostatic stability. Long-range electrostatics were treated using the particle mesh Ewald (PME) method with a 10 Å cutoff for nonbonded interactions. The prepared complex was subjected to a four-stage relaxation protocol. Energy minimization was carried out in two steps: a steepest descent minimization with 5000 steps to remove steric clashes, followed by conjugate gradient minimization with 5000 steps to converge the system to a local potential energy minimum while restraining the protein heavy atoms. Gradual heating from 0 to 298 K was performed over 200 ps under constant-volume (NVT) conditions, using a Langevin thermostat with positional restraints on the protein backbone. Density equilibration was subsequently performed for 500 ps in the NPT ensemble with isotropic Berendsen pressure coupling to adjust solvent density to ~1 $g \cdot cm^{-3}$. Equilibration was extended for 2 ns under constant pressure (1 atm) at 298 K, with progressively reduced harmonic restraints on backbone atoms to allow system relaxation while preserving the overall structural integrity of the protein-ligand complex. Following equilibration, extended-time-scale production simulations were conducted in the isothermal-isobaric ensemble (NPT) at 298.15 K and 1 atm, with periodic boundary conditions. A Langevin thermostat and Berendsen barostat maintained thermal and pressure coupling, respectively. SHAKE constraints were applied to all bonds involving hydrogen atoms, allowing an integration timestep of 2 fs. The production phase was executed for 1000 ns for VEGFR-2D23@PC[n] complexes and 500 ns for DNA@PC[n] systems, restarting seamlessly from the coordinates and velocities of the preceding run. Root-mean-square deviation (RMSD) of the protein/DNA backbone, ligand, and complex was measured, along with the bending angle of the D23 domain (measured through the Val219-Gly220-Tyr221 linker peptide), to assess complex structural stability. The thermodynamics encoded PC[n] binding energy was evaluated using the Molecular Mechanics Generalized Boltzmann Surface area (MM/GBSA[20]) method implemented in Amber23. These analyses were performed on the trajectories saved every 10 ps of the MD simulation files. The binding enthalpies of the VEGFR-2D23@PC[n] and DNA@PC[n] complexes were computed from the most converged trajectories obtained during the RMSD calculations.

4. MM/GBSA binding enthalpy analysis

The MM/GBSA method is an end-point free energy[21] approach that provides an optimal balance between computational efficiency and accuracy[22]. It is widely employed to re-score docked complexes and estimate ligand–target binding affinities using molecular dynamics (MD) simulation trajectories[23]. In this framework, the binding free energy (ΔG_{bind}) of a ligand–target complex is expressed as: $\Delta G_{bind}=\Delta E_{MM} + \Delta G_{sol} - T\Delta S$, where ΔE_{MM} represents the gas-phase molecular mechanics energy, ΔG_{sol} denotes the solvation free energy, and $-T\Delta S$ corresponds to the conformational entropy change upon binding[21]. The molecular mechanics energy (ΔE_{MM}) is calculated using force-field parameters and comprises bonded, electrostatic, and van der Waals interaction energies. The solvation free energy (ΔG_{sol}) is decomposed into polar and nonpolar contributions. The polar solvation component is calculated using the Generalized Born (GB) implicit solvent model, while the nonpolar component is estimated from the solvent-accessible surface area (SASA) using an empirical surface tension term[24,25]. entropy contribution ($-T\Delta S$) can be evaluated using normal-mode or quasi-harmonic analysis[26]. However, these methods are computationally intensive and often introduce significant uncertainty. Therefore, the entropy term is commonly neglected, particularly when comparing relative binding free energies among structurally related ligands targeting the same protein, where entropy contributions are expected to be similar[21,27,28].In this study, the single-trajectory MM/GBSA approach was employed, wherein the ligand, receptor, and complex energies were extracted from the same MD trajectory. This approach minimizes structural noise and improves the consistency of binding free energy estimation by eliminating conformational variability between individual simulations[28]. All MM/GBSA calculations were performed with AmberTools 23.

5. Non-covalent interaction (NCI) analysis

The qualitative estimation of interaction strength was visualised using non-covalent interaction (NCI) analysis performed using the Multiwfn[29] program with previously obtained wavefunction at the level of B3PW91-D3/def2TZVPP.[30] The quantitative indices and electron density characteristics are computed using the AIMALL program.[31] To elucidate the nature of bonded, we evaluated the electron density ($\rho(r)$), Laplacian of electron density ($\nabla^2\rho(r)$), the eigenvalues (λ_1-λ_3) of the electron density in the Hessian matrix, and the associated energy density components, i.e., kinetic (G(r)), potential (v(r)), and the Hamiltonian(K(r)) at the bond critical point (BCP) present at their respective bond path.

6. Energy decomposition and natural orbital analysis

Interaction strength of the PC[1] and the nucleobases was performed using the functional group symmetry adapted perturbation theory (F-SAPT0) method implemented in PSI4 with the jun-cc-pVDZ basis set under the frozen-core approximation.[32,33] Density fitting and a superposition of atomic densities method were applied throughout. The F-SAPT0 decomposition provided group-resolved electrostatic (E_{elec}), exchange (E_{exc}), induction (E_{ind}), and dispersion (E_{disp}) contributions involved in the PC[1]-nucleobase complex formation. The E_{elec} represents the classical Coulombic interaction between the electron densities of the host and guest fragments. The E_{disp} originates from instantaneous density fluctuations that give rise to long-range correlation forces. The E_{ind} reflects donor-acceptor mixing, arising when occupied orbitals of one fragment overlap with the

unoccupied orbitals of the other. Finally, the E_{exc} accounts for the destabilization imposed by the Pauli exclusion principle, which prevents electrons of identical spin from occupying the same spatial region.

The change in electronic polarization of fragment PC[1] due to the presence of fragment nucleobase is essentially expressed as

$$\Delta\rho_{PC[1]}(r) = \rho^{PC[1]@NB}_{PC[1]} - \rho^{isolated\ PC[1]}_{PC[1]}(r) \quad (1)$$

$$\Delta\rho_{NB}(r) = \rho^{PC[1]@NB}_{NB} - \rho^{isolated\ NB}_{NB}(r) \quad (2)$$

$$\Delta\rho_{PC[1]@NB}(r) = \rho^{PC[1]@NB}_{PC[1]} - \rho^{isolated\ PC[1]}_{PC[1]}(r) + \rho^{PC[1]@NB}_{NB} - \rho^{isolated\ NB}_{NB}(r)$$

$$= \rho^{PC[1]@NB}_{PC[1]} + \rho^{PC[1]@NB}_{NB} - \rho^{isolated\ PC[1]}_{PC[1]}(r) - \rho^{isolated\ NB}_{NB}(r)$$

$$\Delta\rho_{PC[1]@NB}(r) = \rho^{PC[1]@NB}_{PC[1]@NB} - \rho^{isolated\ PC[1]}_{PC[1]}(r) - \rho^{isolated\ NB}_{NB}(r) \quad (3)$$

Equation (1) and (2) depicts the change in electron density of individual fragment PC[1] and nucleobases (NB) due to the presence of their complementary fragments in the PC[1]-nucleobase complex systems. Equation (3) provides the charge transfer polarization, which is visualized using ChemCraft[34] program package at a contour value of 0.001 atomic units. Further to reinforce the E_{ind}, natural bond orbital (NBO) analysis was performed, and the second-order perturbation energy E(2) quantifies the stabilization associated with donor-acceptor delocalization, with larger values reflecting stronger orbital overlap and charge transfer.[35,36]

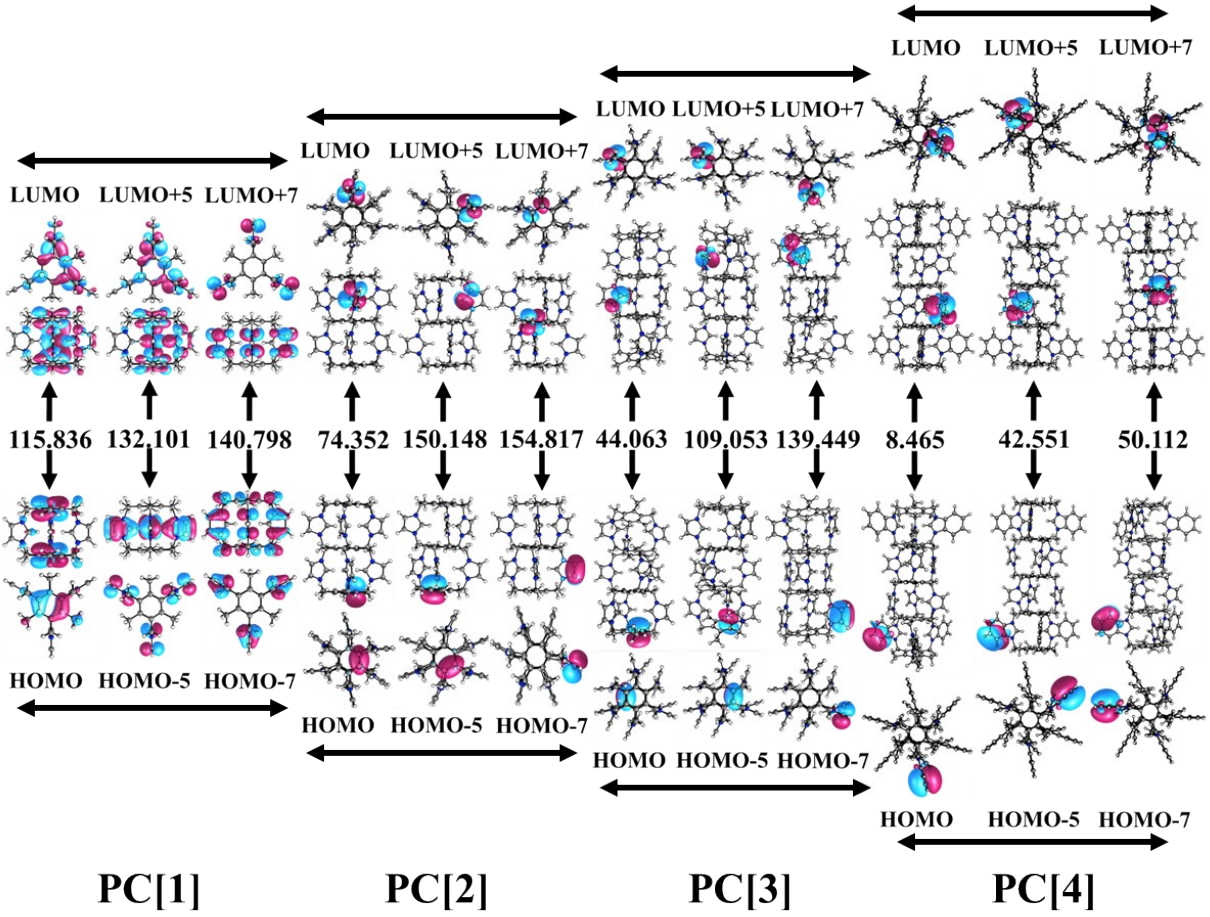

Figure S1. Frontier Molecular Orbital (FMO) diagram of PC[n] (n = 1-4) shown from the front (top) and side (bottom) views, depicting variations in HOMO→LUMO, HOMO-5→LUMO+5, and HOMO-7→LUMO+7 energy gaps (ΔE_{gap}) and orbital distributions. The ΔE_{gap} is presented in kcal.mol^{-1}. All orbitals are visualized at an isosurface value of 0.03 a.u.

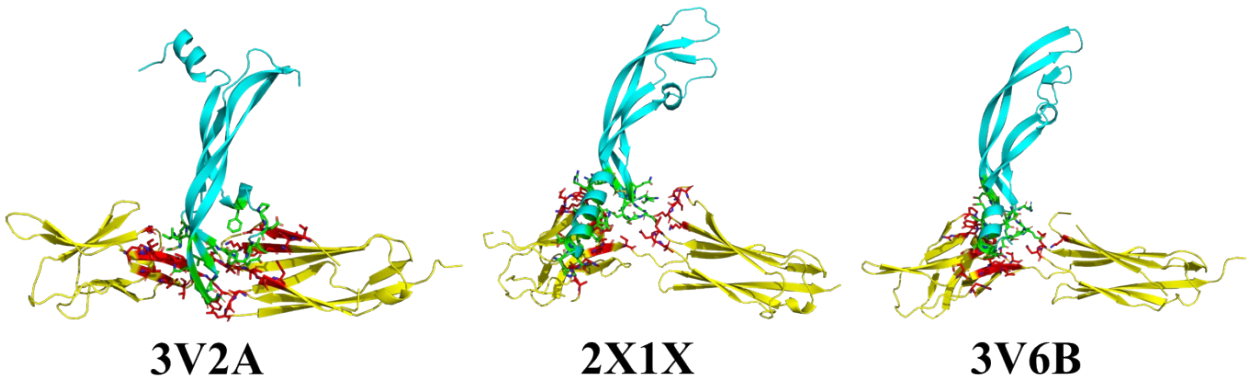

Figure S2. Crystal structures of VEGF-A (PDB ID: 3V2A), VEGF-C (PDB ID: 2X1X), and VEGF-E (PDB ID: 3V6B) in complex with the VEGFR-2D23 domain. The red regions represent the interacting residues of the VEGFR-2D23 receptor, while the green regions indicate the participating residues of VEGF-A, VEGF-C, and VEGF-E that mediate binding with VEGFR-2D23.

Table S1. Residues of VEGF-A and VEGFR-2D23 are involved in complex formation, along with their buried accessible surface areas (ASAs) and respective percentage contributions to the interaction interface.

3V2A (VEGFR-2D23@VEGF-A)		
Residue	Buried ASA (Å^2)	Buried ASA (%)
His133	27.8	24.4
Val135	28.7	40.4
Tyr137	37.2	25.3
Thr139	1.1	1.8
Ala195	6.2	68.8
Gly196	10.4	30.9
Val216	11.9	85.8
Val217	44.6	100
Val218	16.3	41.4
Val219	48.5	87.1
Gly220	15.3	99.1
Tyr221	9.8	15.2
Asn253	18.9	27.6
Val254	5	81.6
Gly255	38.5	93.8
Ile256	35.6	98.9
Asp257	25.3	29.5
Phe258	16.8	44.1
Val273	15.2	13.5
Asn274	48	65.1
Arg275	26.2	46.1
Asp276	28.9	40.1
Lys286	4.6	8.5
Phe288	26.4	90.6
Leu289	0.7	1.7
Ser311	13.5	91.2
Gly312	19.2	32
Leu313	35.3	24.7

Table S2. Residues of VEGF-C and VEGFR-2D23 are involved in complex formation, along with their buried accessible surface areas (ASAs) and respective percentage contributions to the interaction interface.

2X1X (VEGFR-2D23@VEGF-C)		
Residue	**Buried ASA (Å^2)**	**Buried ASA (%)**
Asp131	0.5	0.9
Gln132	78.1	52.7
His133	34.3	33.6
Arg164	16.6	26.7
Tyr165	109.1	86
Pro166	24.3	27
Glu167	1.4	1.3
Lys168	7.8	9.5
Ser193	26.6	56.1
Tyr194	49	72.7
Ala195	10.4	100
Gly196	39.1	99.2
Met197	51.5	97.8
Met213	21.6	30.1
Ile215	32.7	37.4
Val216	4.9	29.7
Val218	24.3	43.9
Leu252	54.1	64
Asn253	52.9	61.7
Val254	1.3	28.9
Gln280	14.3	14.6
Gly282	18.8	43.4
Ser283	9.2	15.3
Glu284	34.1	26.6
Lys286	27.1	34.7

Table S3. Residues of VEGF-E and VEGFR-2D23 are involved in complex formation, along with their buried accessible surface areas (ASAs) and respective percentage contributions to the interaction interface.

3V6B (VEGFR-2D23@VEGF-E)		
Residue	**Buried ASA (Å^2)**	**Buried ASA (%)**
His133	0.5	0.5
Ile138	1.5	31.6
Lys142	2.1	4.7
Arg164	4.8	7.5
Tyr165	97.9	69.2
Pro166	52.7	56.3
Ser193	40.1	85.3
Tyr194	60.2	71.9
Ala195	6.7	100
Gly196	40.5	84.7
Met197	27.9	69.8
Met213	5.5	6.9
Ile215	34.1	50.4
Val216	17.7	76.5
Val217	0.5	1
Val218	38.2	65
Leu252	50.8	55.5
Asn253	51.9	69.1
Lys286	24.6	34.9

Table S4. Residues of VEGFR-2D23 are involved in complex formation with PC[2], along with their interacting residue atoms and their corresponding distances in Å units.

VEGFR-2D23@PC[2]					
Residue	**Protein atom**	**Distance (Å)**	**Residue**	**Protein atom**	**Distance (Å)**
Glu140	OE1	3.63	Gly282	O	3.75
Glu140	CD	3.84	Gly282	O	3.91
Glu140	OE1	2.85	Gly282	O	3.71
Glu140	OE1	3.69	Ser283	O	3.91
Glu140	OE2	3.94	Glu284	OE2	3.02
Glu140	OE1	3.12	Glu284	CD	3.74
Glu140	OE1	3.45	Glu284	OE1	3.47
Glu140	OE1	3.48	Glu284	OE2	3.19
Glu140	CD	3.25	Glu284	OE2	3.93
Glu140	OE1	2.74	Glu284	CG	3.95
Glu140	OE2	3.46	Glu284	OE2	3.26
Glu140	OE1	3.11	Glu284	CD	3.87
Glu140	CG	3.92	Glu284	OE1	3.92
Glu140	OE1	3.95	Glu284	OE2	3.18
Glu140	CG	3.96	Glu284	OE1	3.47
Glu140	OE1	3.76	Glu284	CD	3.76
Glu140	CD	3.8	Glu284	OE1	3.66
Glu140	OE1	2.88	Glu284	OE2	3.04
Glu140	CD	3.91	Glu284	CD	3.81
Glu140	OE1	2.88	Glu284	OE1	3.13
Glu140	O	3.76	Glu284	OE2	3.7
Glu140	CD	3.72	Glu284	CG	3.75
Glu140	OE1	3.47	Glu284	CD	3.61
Glu140	OE2	3.99	Glu284	OE2	3.58
Ser193	OG	3.64	Glu284	CD	3.86
Ser193	O	3.78	Glu284	OE2	2.78
Ser193	OG	3.66	Glu284	OE2	3.52
Ser193	C	3.93	Glu284	CD	3.71
Ser193	O	4	Glu284	OE2	3
Ser193	CB	3.86	Glu284	OE2	3.16
Ser193	OG	2.87	Glu284	OE2	3.76
Ser193	OG	3.76			

*CD, CG denote carbon atoms in side-chain positions, and OE1/OE2 refer to the two oxygen atoms of a glutamate (Glu) carboxylate group.

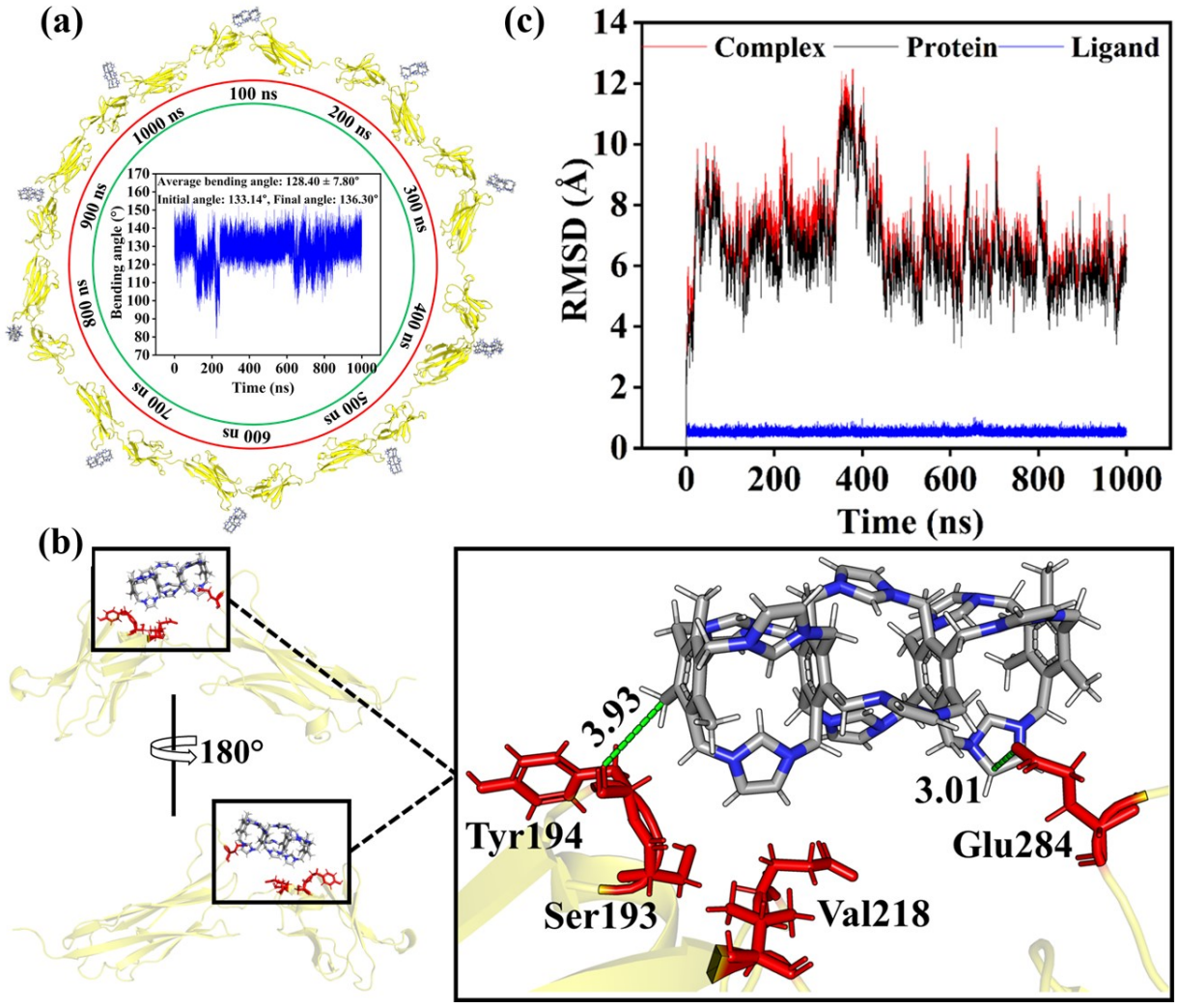

Figure S3. MD simulation analysis of the VEGFR-2 D2–D3 domain complexed with the ligand. (a) Time-resolved conformational transitions of VEGFR-2@PC[3] over a 1000 ns MD trajectory, with the inner plot depicting the bending angle fluctuation, (b) Binding interface of the PC[3] with VEGFR-2, highlighting key interacting residues and hydrogen bond distances in Å. The left panel shows 180° opposite views of the complex for spatial clarity. (d) RMSD plots of the VEGFR-2@PC[3] complex, free protein, and ligand over 1000 ns, illustrating structural stability and equilibration throughout the simulation.

Table S5. Residues of VEGFR-2D23 involved in complex formation with PC[3], along with their interacting residue atoms and their corresponding distances in Å units.

VEGFR-2D23@PC[3]					
Residue	**Protein atom**	**Distance (Å)**	**Residue**	**Protein atom**	**Distance (Å)**
Glu284	OE2	3.71	Glu284	OE2	3.18
Glu284	OE2	3.83	Glu284	CB	3.89
Glu284	OE2	3.18	Glu284	CD	3.94
Glu284	OE2	3.19	Glu284	OE2	3.02
Glu284	CD	3.72	Glu284	CD	3.99
Glu284	OE1	3.53	Glu284	OE2	3.01
Glu284	OE2	3.14	Tyr194	O	3.93
Glu284	OE2	3.39			

*OE1/OE2 denote carboxylate oxygens of acidic residues (Glu), while CB, CG, and CD represent the β-, γ-, and δ-carbon atoms in amino-acid side chains.

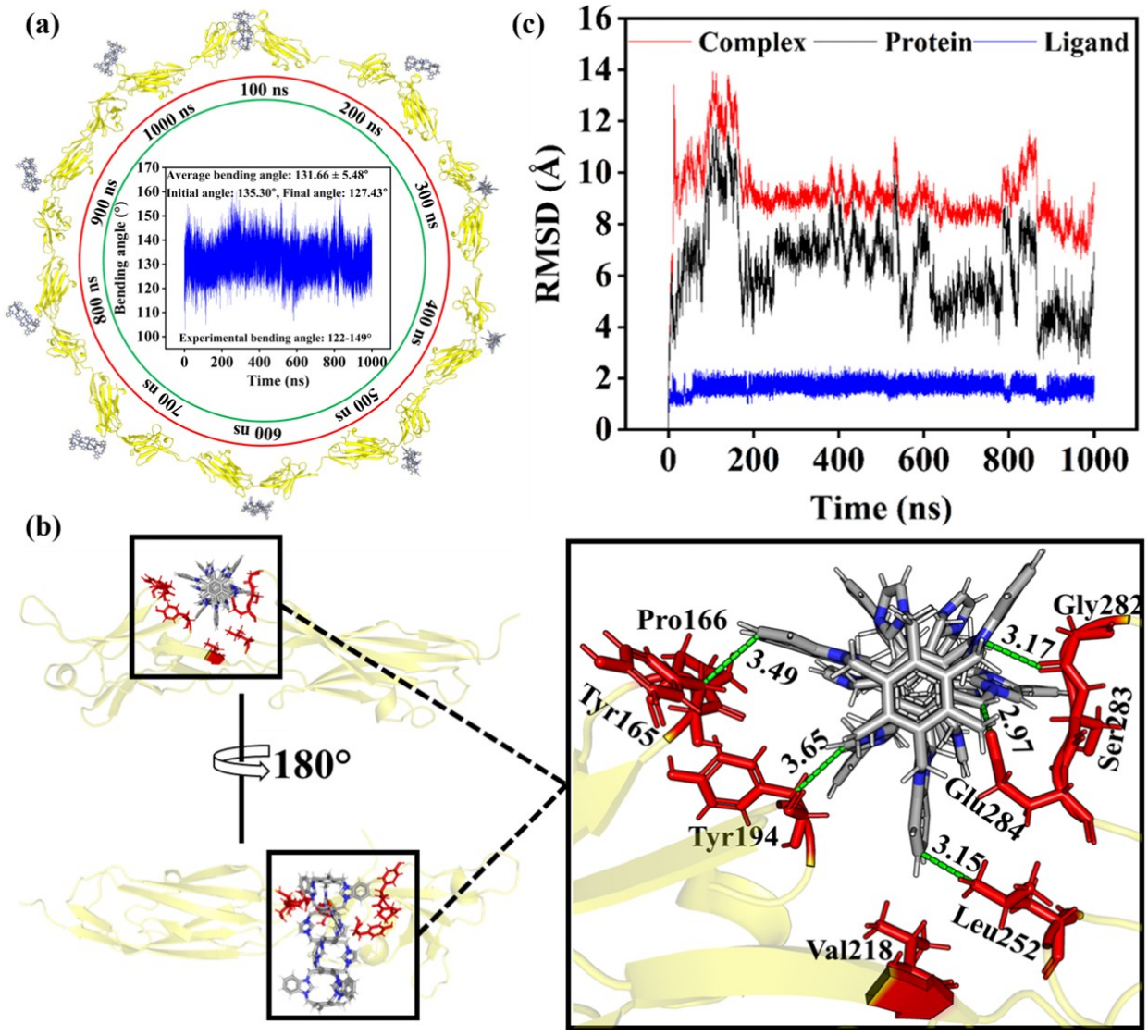

Figure S4. MD simulation analysis of the VEGFR-2 D2-D3 domain complexed with the ligand. (a) Time-resolved conformational transitions of VEGFR-2@PC[4] over a 1000 ns MD trajectory, with the inner plot depicting the bending angle fluctuation, (b) Binding interface of the PC[4] with VEGFR-2, highlighting key interacting residues and hydrogen bond distances in Å. The left panel shows 180° opposite views of the complex for spatial clarity. (d) RMSD plots of the VEGFR-2@PC[4] complex, free protein, and ligand over 1000 ns, illustrating structural stability and equilibration throughout the simulation.

Table S6. Residues of VEGFR-2D23 are involved in complex formation with PC[4], along with their interacting residue atoms and their corresponding distances in Å units.

VEGFR-2D23@PC[4]					
Residue	**Protein atom**	**Distance (Å)**	**Residue**	**Protein atom**	**Distance (Å)**
Tyr165	CB	3.49	Glu284	CG	3.62
Tyr165	C	3.95	Glu284	CD	3.75
Tyr165	O	3.92	Glu284	OE2	3.67
Tyr165	CB	3.57	Glu284	OE2	3.45
Tyr194	CB	3.71	Glu284	CG	3.83
Tyr194	CA	3.99	Glu284	CD	3.19
Tyr194	O	3.85	Glu284	OE1	3.44
Tyr194	CB	3.65	Glu284	OE2	3.18
Leu252	CD2	3.63	Glu284	OE2	3.66
Leu252	CD2	3.15	Glu284	CD	3.55
Leu252	CD2	3.98	Glu284	OE1	3.17
Gly282	O	3.31	Glu284	OE2	2.97
Gly282	CA	3.66	Glu284	CG	3.84
Gly282	C	3.99	Glu284	CD	3.4
Gly282	O	3.17	Glu284	OE2	3.02
Gly282	O	3.25	Glu284	OE2	3.54
Gly282	O	3.87	Glu284	CG	3.76
Gly282	CA	3.56	Glu284	CD	3.57
Gly282	C	3.89	Glu284	OE1	3.79
Gly282	O	3.42	Glu284	OE2	3.96
Gly282	O	3.26	Glu284	CG	3.67
Gly282	O	3.63	Glu284	CD	3.94
Gly282	CA	3.3	Glu284	CD	3.45
Gly282	O	3.7	Glu284	OE1	3.25
Glu284	CG	3.69	Glu284	OE2	3.38
Glu284	OE2	3.46			

*CA, CB, CG, and CD/ CD2 denote the α-, β-, γ-, and δ-carbons of amino-acid residues; C and O refer to the backbone carbonyl carbon and oxygen; and OE1/OE2 are the two carboxylate oxygens of acidic residues such as Glu.

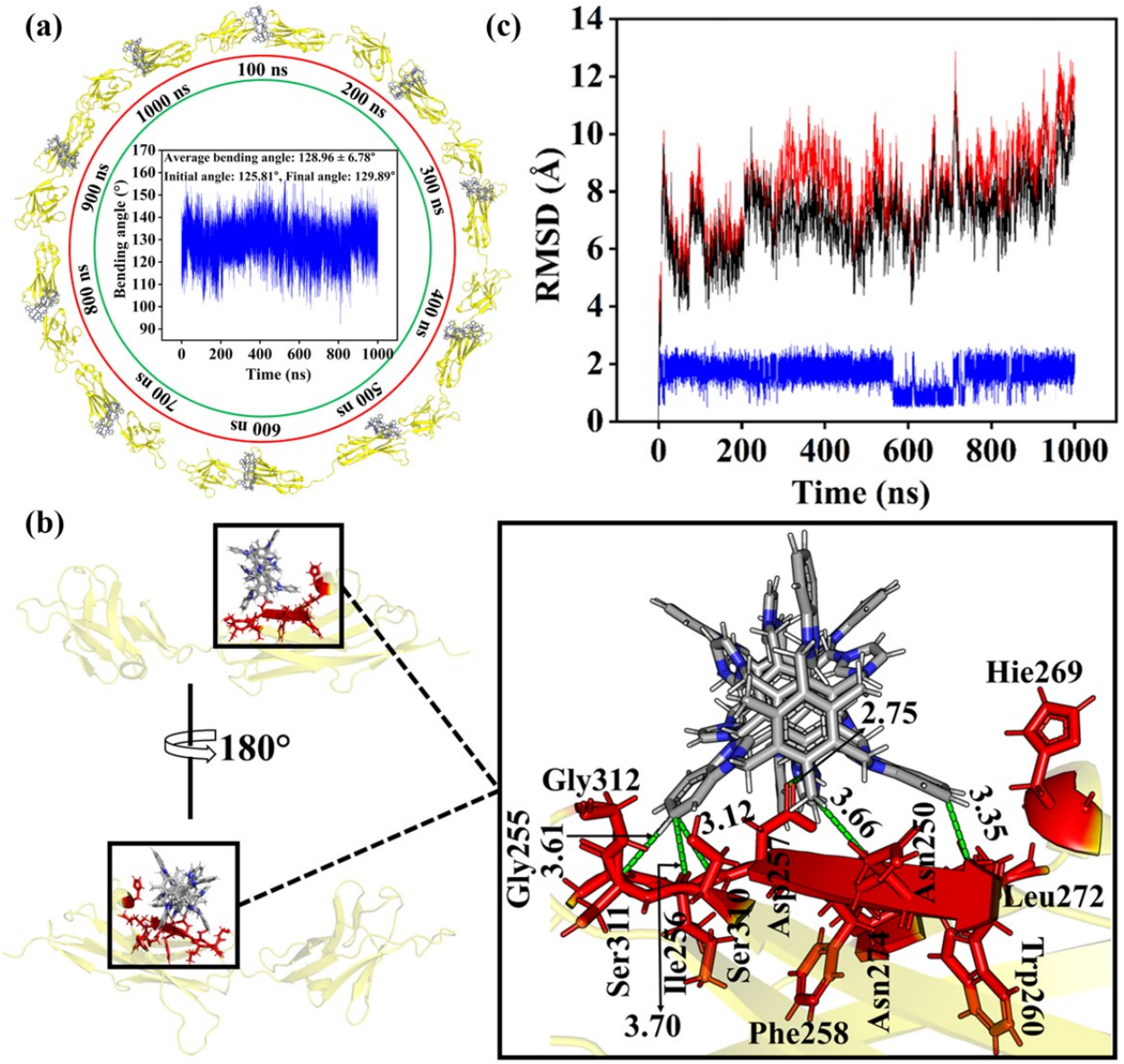

Figure S5. MD simulation analysis of the double alanine-mutated VEGFR-2 D2-D3 domain complexed with the ligand. (a) Time-resolved conformational transitions of VEGFR-2@PC[4] over a 1000 ns MD trajectory, with the inner plot depicting the bending angle fluctuation, (b) Binding interface of the PC[4] with VEGFR-2, highlighting key interacting residues and hydrogen bond distances in Å. The left panel shows 180° opposite views of the complex for spatial clarity. (d) RMSD plots of the VEGFR-2@PC[4] complex, free protein, and ligand over 1000 ns, illustrating structural stability and equilibration throughout the simulation.

Table S7. Residues of double alanine mutated VEGFR-2D23 involved in complex formation with PC[4], along with their interacting residue atoms and their corresponding distances in Å units.

M-VEGFR-2D23@PC[4]					
Residue	**Protein atom**	**Distance (Å)**	**Residue**	**Protein atom**	**Distance (Å)**
Gly255	O	3.61	Asp257	CG	3.12
Gly255	C	3.87	Asp257	OD1	2.75
Gly255	O	3.75	Asp257	OD2	3.03
Ile256	CA	3.88	Asp257	CG	3.87
Ile256	C	3.7	Asp257	OD1	2.82
Ile256	N	3.88	Asp257	CG	3.88
Ile256	C	3.79	Asp257	OD1	3.07
Ile256	O	3.79	Asp257	OD2	3.94
Asp257	CB	3.49	Asp257	CB	3.58
Asp257	CB	3.89	Asp257	OD1	3.55
Asp257	CG	3.49	Asp257	CB	3.35
Asp257	OD1	3.24	Asp257	OD1	3.63
Asp257	N	3.76	Asp257	CG	3.91
Asp257	CB	3.96	Asp257	OD1	3.07
Asp257	CB	3.67	Asp257	OD1	3.93
Asp257	CG	3.92	Asp257	OD1	3.51
Asp257	OD1	3.22	Asp257	OD1	3.72
Asp257	OD1	3.86	Phe258	O	3.95
Asp257	CG	3.88	Phe258	O	3.66
Asp257	OD1	2.99	Phe258	O	3.95
Asp257	CG	3.93	Phe258	O	3.89
Asp257	OD1	3.06	Leu272	CD1	3.35
Asp257	OD1	3.73	Leu272	CD1	3.55
Asp257	OD2	3.97	Ser310	O	3.26
Asp257	OD1	3.2	Ser310	O	3.12
Asp257	OD1	3.91			

*CA, CB, CG, CD1/CD2 denote α-, β-, γ-, and δ-carbons of residue side chains; C, O, and N refer to backbone atoms; and OD1/OD2 are the carboxylate oxygens of Asp residues.

Table S8. MM/GBSA binding free energy analysis of VEGFR-2D23 and its mutant (M-VEGFR-2D23M) in complex with PC[n], (n = 2-4). Reported values are in kcal·mol^{-1}. ΔE_{vdW} and $\Delta E_{non\text{-}polar}$ denote dispersion and hydrophobic contributions, respectively, while ΔE_{elec} and ΔE_{polar} correspond to electrostatic interactions and polar solvation energies. The total enthalpy (ΔH_{total}) reflects the overall binding strength, revealing strong dispersion-driven stabilization in PC[4] and its attenuation upon double mutation, consistent with the loss of key interfacial contacts.

Energy Components	VEGFR-2 D23@ PC[2]	VEGFR-2D23@ PC[3]	VEGFR-2 D23@ PC[4]	M-VEGFR-2D23@PC[4]
ΔE_{vdW}	-21.0 ± 4.0	-17.9 ± 3.6	-32.8 ± 3.5	-20.4 ± 3.7
ΔE_{elec}	198.0 ± 33.3	272.7 ± 43.9	654.6 ± 43.4	675.2 ± 48.3
ΔE_{polar}	-178.1 ± 33.1	-255.3 ± 43.8	-616.7 ± 42.7	-642.6 ± 47.8
$\Delta E_{non\text{-}polar}$	-40.6 ± 5.8	-43.5 ± 5.5	-53.3 ± 3.1	-36.5 ± 5.6
ΔH_{total}	-47.7 ± 6.2	-43.9 ± 6.5	-48.3 ± 3.5	-24.3 ± 5.8

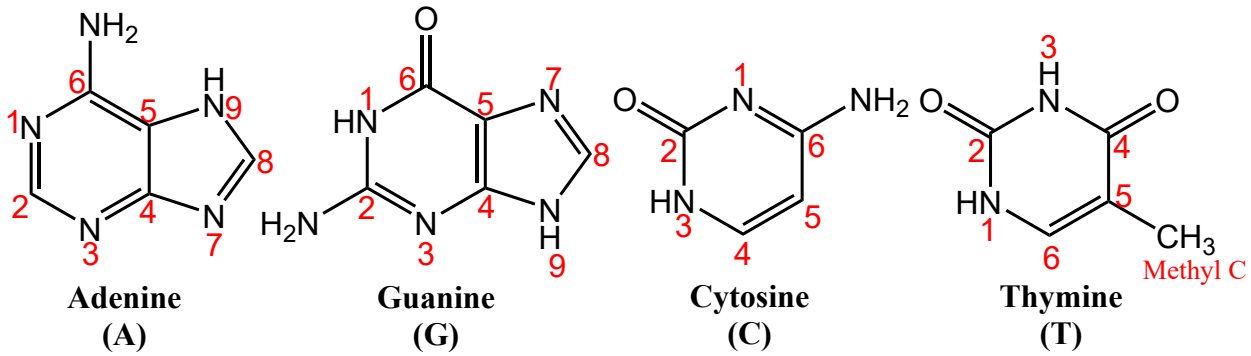

Scheme S1. Structure and numbering of the nucleobases considered in this study.

Table S9. The nucleotides of the duplex DNA involved in complex formation with PC[2], along with their interacting atoms and their corresponding distances in Å units.

Nucleotides	Interacting domain duplex DNA…PC[2]	Distance (Å)
DC4	C2(=O)...H-C	2.95
DG5	Sugar(O)… H-C	2.76
DG5	Sugar(H)…N-C	2.42
DA6	Phosphate(O)… H-C	2.45/2.50
DA6	Phosphate(=O)… H-C	2.50
DA6	Sugar(H)…N-C	2.68
DG25	Phosphate(=O)… H-C	2.51/2.67

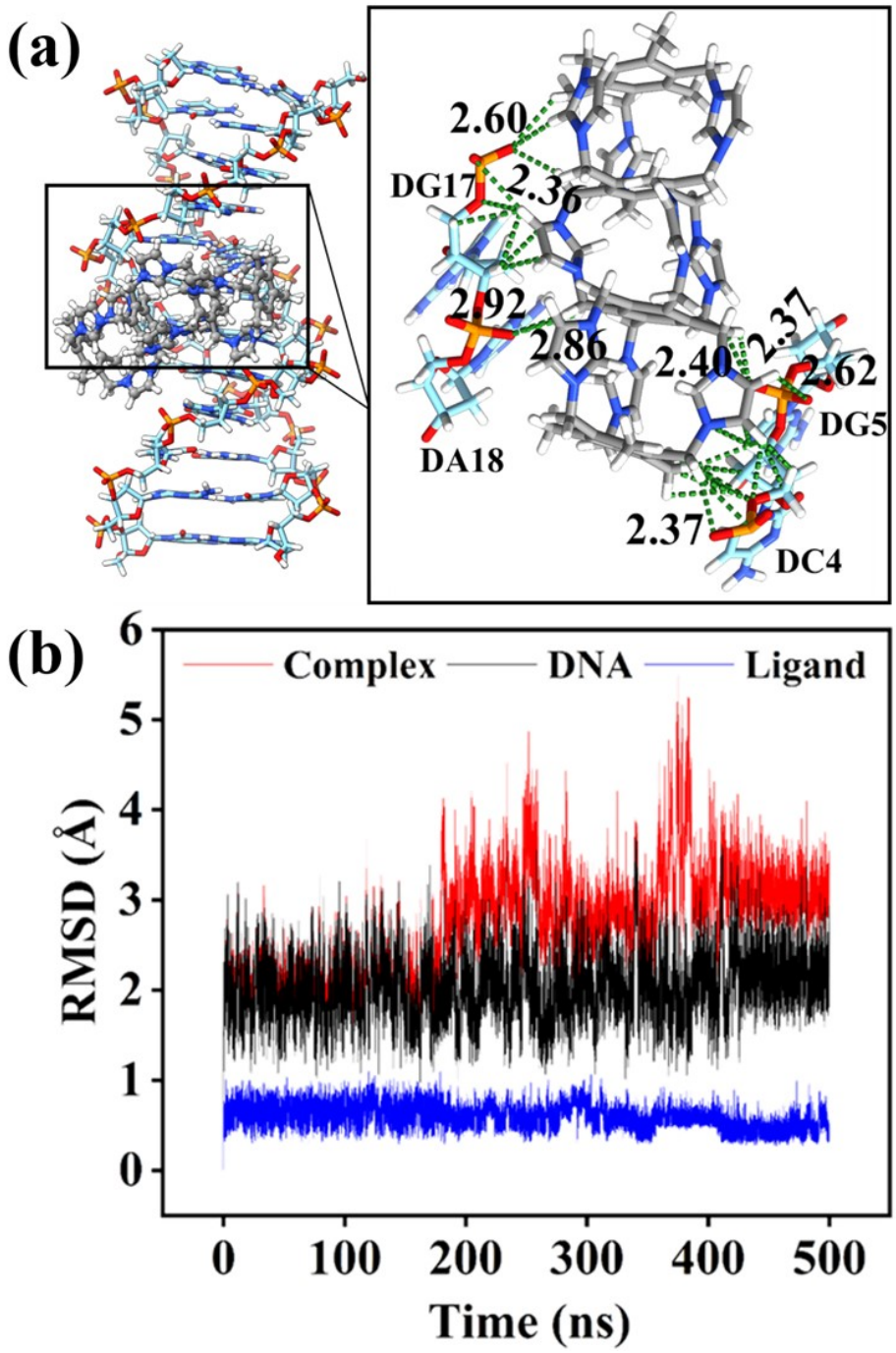

Figure S6. MD simulation analysis of the DNA@PC[3] complex. (a) Structural representation of the ligand bound within the DNA double helix, highlighting key hydrogen-bonding interactions with nucleobases. The inset shows the overall orientation of DNA@PC[3] binding, highlighting the groove-specific interaction mode. (b) RMSD profiles of the complex, DNA, and PC[3] over a 500 ns MD trajectory, demonstrating the conformational stability of the DNA backbone and the sustained binding of the ligand throughout the simulation.

Table S10. The nucleotides of the duplex DNA involved in complex formation with PC[3], along with their interacting atoms and their corresponding distances in Å units.

Nucleotides	Interacting domain duplex DNA…PC[3]	Distance (Å)
DC4	Phosphate(=O)…H-C	2.37/3.04
DG5	Phosphate(=O)…H-C	2.37/2.40/2.62
DG17	Phosphate(=O)…H-C	2.36/2.60
DA18	Phosphate(=O)…H-C	2.86/2.92

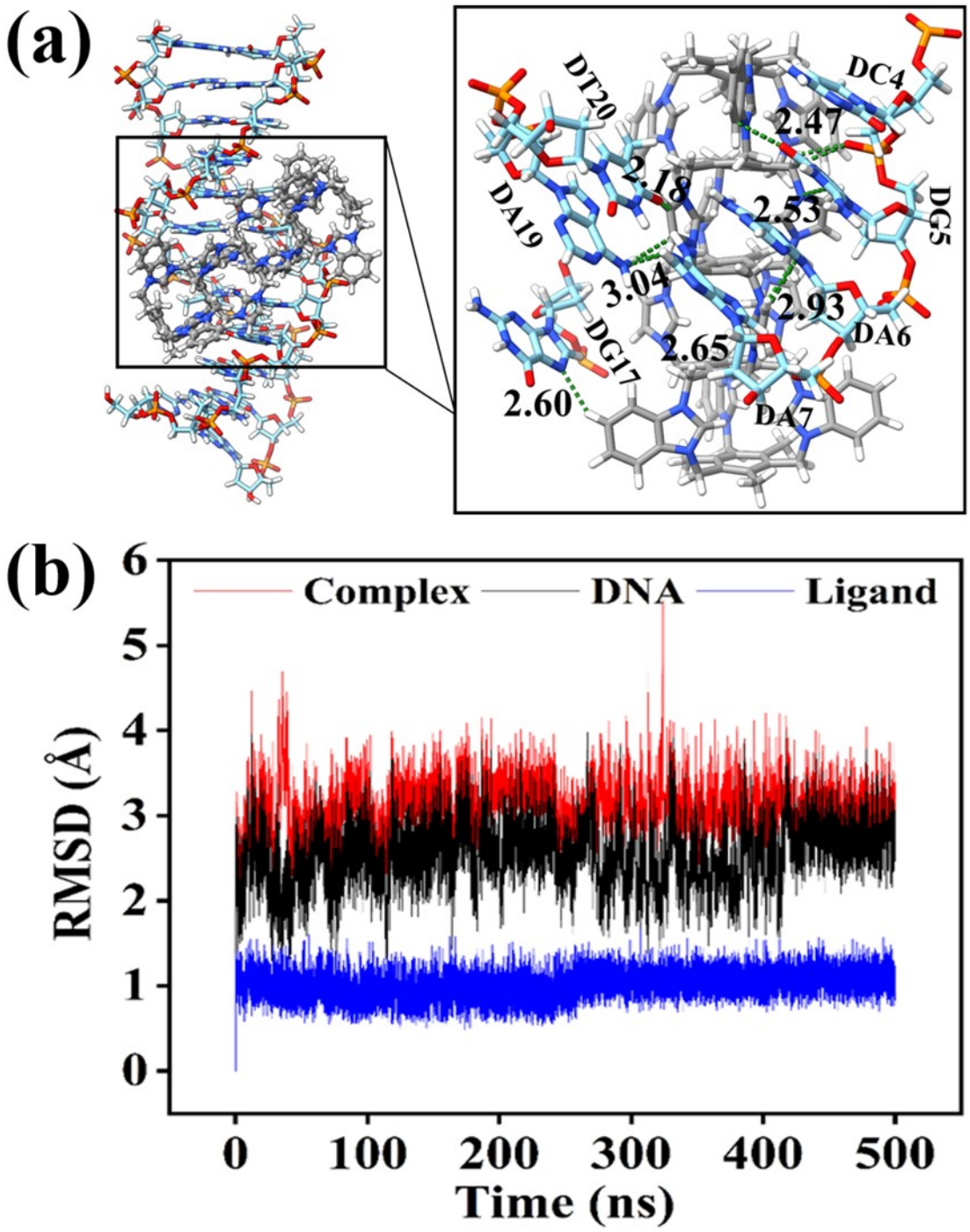

Figure S7. MD simulation analysis of the DNA@PC[4] complex. (a) Structural representation of the ligand bound within the DNA double helix, highlighting key hydrogen-bonding interactions with nucleobases. Distances are given in Å. The inset shows the overall orientation of DNA@PC[4] binding, highlighting the groove-specific interaction mode. (b) RMSD profiles of the complex, DNA, and PC[4] over a 500 ns MD trajectory, demonstrating the conformational stability of the DNA backbone and the sustained binding of the ligand throughout the simulation.

Table S11. The nucleotides of the duplex DNA involved in complex formation with PC[4], along with their interacting atoms and their corresponding distances in Å units.

Nucleotides	Interacting domain duplex DNA…PC[4]	Distance (Å)
DC4	$\pi_{pyrimidine}\cdots\pi_{phenyl}$	5.24
DG5	Phosphate(=O)…H-C	2.47
DG5	N7…H-C	2.71
DG5	C8H…N-C	2.53
DA6	N7… H-C	2.93
DA7	Phosphate(=O)…H-C	2.65
DG17	Phosphate(=O)…H-C	2.53
DA9	N7… H-C	3.04
DT20	C4(=O)…H-C	2.18

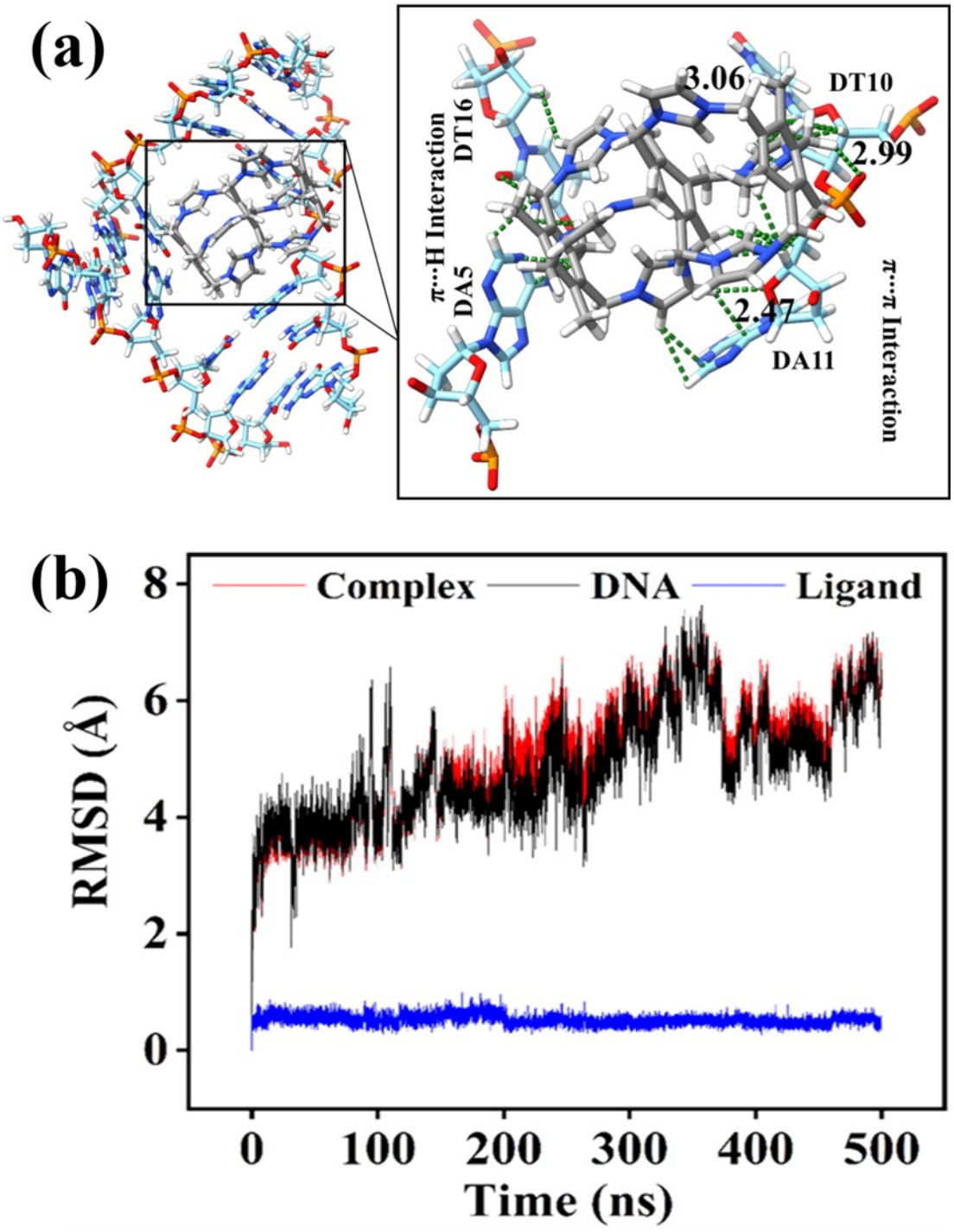

Figure S8. MD simulation analysis of the fork DNA@PC[2] complex. (a) Structural representation of the ligand bound within the DNA double helix, highlighting key hydrogen-bonding interactions with nucleobases. Distances are given in Å. The inset shows the overall orientation of DNA@PC[2] binding, highlighting the groove-specific interaction mode. (b) RMSD profiles of the complex, DNA, and PC[2] over a 500 ns MD trajectory.

Table S12. The nucleotides of the fork DNA involved in complex formation with PC[2], along with their interacting atoms and their corresponding distances in Å units.

Nucleotides	Interacting domain fork DNA…PC[2]	Distance (Å)
DA5	$\pi_{pyrimidine}$…H-C	3.70
DA5	$\pi_{imidazole}$…H-C	5.07
DT10	C2(=O)…H-C	3.06
DA11	Phosphate(=O)…H-C	2.99
DA11	$\pi_{pyrimidine}$…$\pi_{imidazole}$	5.02
DA11	Sugar(O)…H-C	2.47
DT16	$\pi_{pyrimidine}$…$\pi_{imidazole}$	5.79
DT16	$\pi_{pyrimidine}$…H-C	5.24

Table S13. MM/GBSA binding free energy analysis of duplex DNA and fork DNA (3WJ) in complex with PC[n], (n = 2-4). Reported values are in kcal·mol^{-1}. ΔE_{vdW} and $\Delta E_{non\text{-}polar}$ denote dispersion and hydrophobic contributions, respectively, while ΔE_{elec} and ΔE_{polar} correspond to electrostatic interactions and polar solvation energies. The total enthalpy (ΔH_{total}) reflects the overall binding strength, revealing strong dispersion-driven stabilization in PC[4] and its attenuation upon double mutation, consistent with the loss of key interfacial contacts.

Energy Components	duplex DNA@ PC[2]	duplex DNA@ PC[3]	duplex DNA@ PC[4]	Fork 3WJ@ PC[2]
ΔE_{vdW}	-29.8 ± 4.7	-19.9 ± 4.1	-62.1 ± 4.3	-34.5 ± 3.5
ΔE_{elec}	-2825.1 ± 67.1	$-4163. \pm 174.2$	$-5873. \pm 65.5$	-2514.2 ± 48.9
ΔE_{polar}	2831.8 ± 68.7	4168.5 ± 178.4	5895.7 ± 66.5	2505.7 ± 48.0
$\Delta E_{non\text{-}polar}$	-2.9 ± 0.5	-2.0 ± 0.5	-5.3 ± 0.3	-3.2 ± 0.2
ΔH_{total}	-26.0 ± 5.3	-17.0 ± 4.6	-44.8 ± 3.8	-46.3 ± 4.5

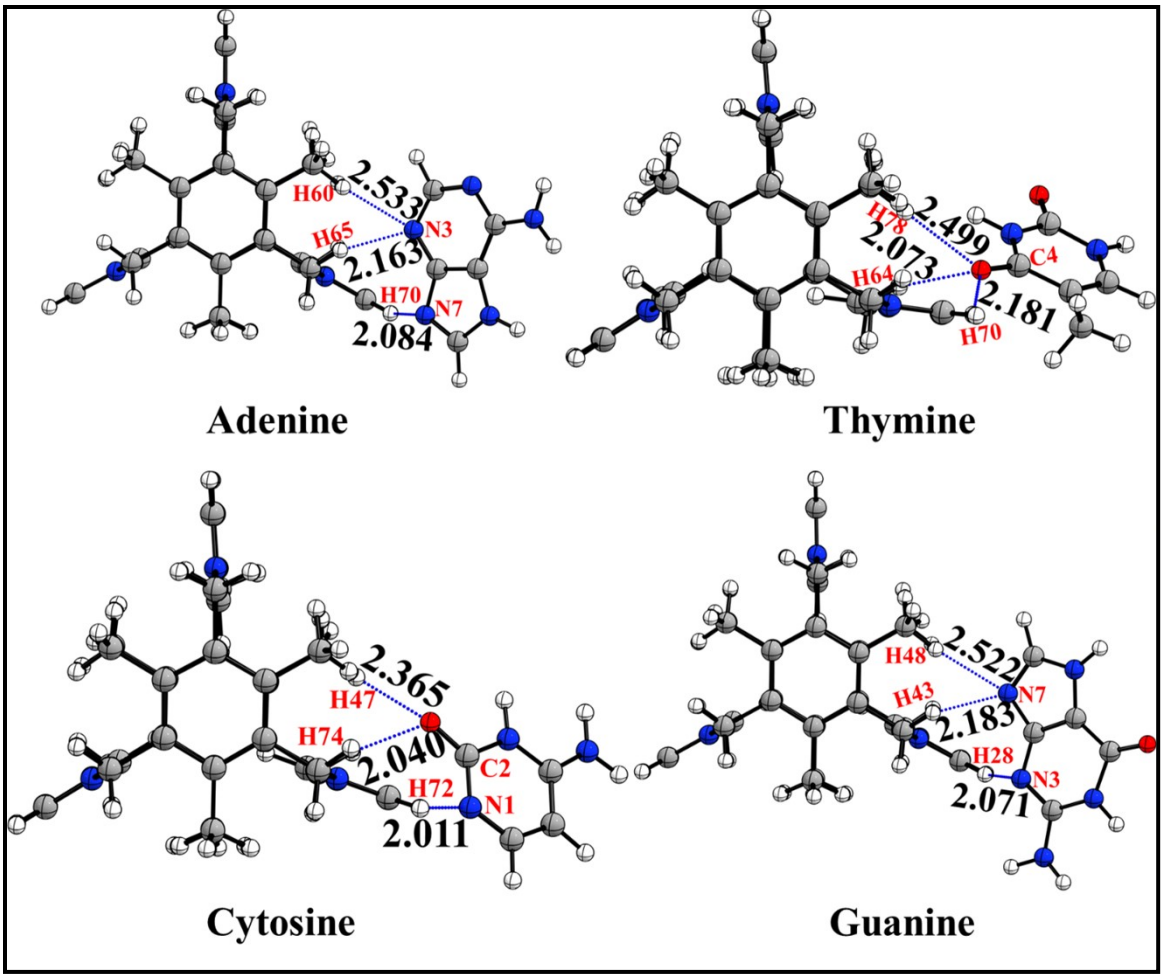

Figure S9. Optimized geometries of PC[1] complexes with DNA nucleobases-adenine, thymine, cytosine, and guanine-computed at the DFT level. The structures display the preferred binding conformations and key noncovalent interactions, including hydrogen bonds and electrostatic contacts between the macrocyclic PC[1] cavity and nucleobase donor/acceptor sites. Interaction distances (in Å units) are indicated, highlighting base-specific recognition patterns that govern binding strength and orientation.

Table 14. Binding energies (ΔE_b), zero-point energy-corrected binding energies ($\Delta E_{b\text{-}ZPE}$), BSSE-corrected binding energies ($\Delta E_{b\text{-}BSSE}$), Gibbs free energies (ΔG), and enthalpies (ΔH) of PC[1]–nucleobase (A, T, C, G) complexes calculated using different DFT-D3 functionals (PBE0, BLYP, M06-2X, TPSS, and CAM-B3LYP). All energies are given in kcal·mol^{-1}.

Systems	**PBE0**				
	ΔE_b	**$\Delta E_{b\text{-}ZPE}$**	**$\Delta E_{b\text{-}BSSE}$**	**ΔG**	**ΔH**
PC[1]@adenine	-38.905	-37.277	-39.650	-25.380	-36.585
PC[1]@thymine	-24.009	-22.950	-26.060	-11.384	-22.535
PC[1]@cytosine	-43.672	-41.911	-45.330	-29.645	-41.337
PC[1]@guanine	-30.731	-29.932	-31.950	-17.968	-29.339
			BLYP		
PC[1]@adenine	-38.134	-37.046	-39.210	-24.353	-36.517
PC[1]@thymine	-24.149	-22.992	-25.950	-10.772	-22.619
PC[1]@cytosine	-42.939	-41.092	-44.200	-28.263	-40.529
PC[1]@guanine	-30.477	-29.539	-31.440	-16.747	-29.014
			M06-2X		
PC[1]@adenine	-41.048	-39.211	-42.010	-26.278	-38.576
PC[1]@thymine	-23.411	-22.525	-25.310	-11.617	-21.989
PC[1]@cytosine	-43.175	-41.561	-44.750	-30.328	-40.798
PC[1]@guanine	-30.516	-29.953	-31.670	-18.550	-29.134
			TPSS		
PC[1]@adenine	-38.048	-37.198	-39.650	-25.114	-36.641
PC[1]@thymine	-23.751	-22.824	-25.700	-11.449	-22.358
PC[1]@cytosine	-42.886	-41.234	-44.430	-29.060	-40.617
PC[1]@guanine	-30.324	-29.493	-31.520	-17.324	-28.964
			CAM-B3LYP		
PC[1]@adenine	-38.852	-37.115	-39.420	-25.355	-36.398
PC[1]@thymine	-24.450	-23.260	-26.440	-11.383	-22.893
PC[1]@cytosine	-44.102	-42.199	-45.690	-30.037	-41.640
PC[1]@guanine	-30.966	-30.167	-32.030	-18.580	-29.484

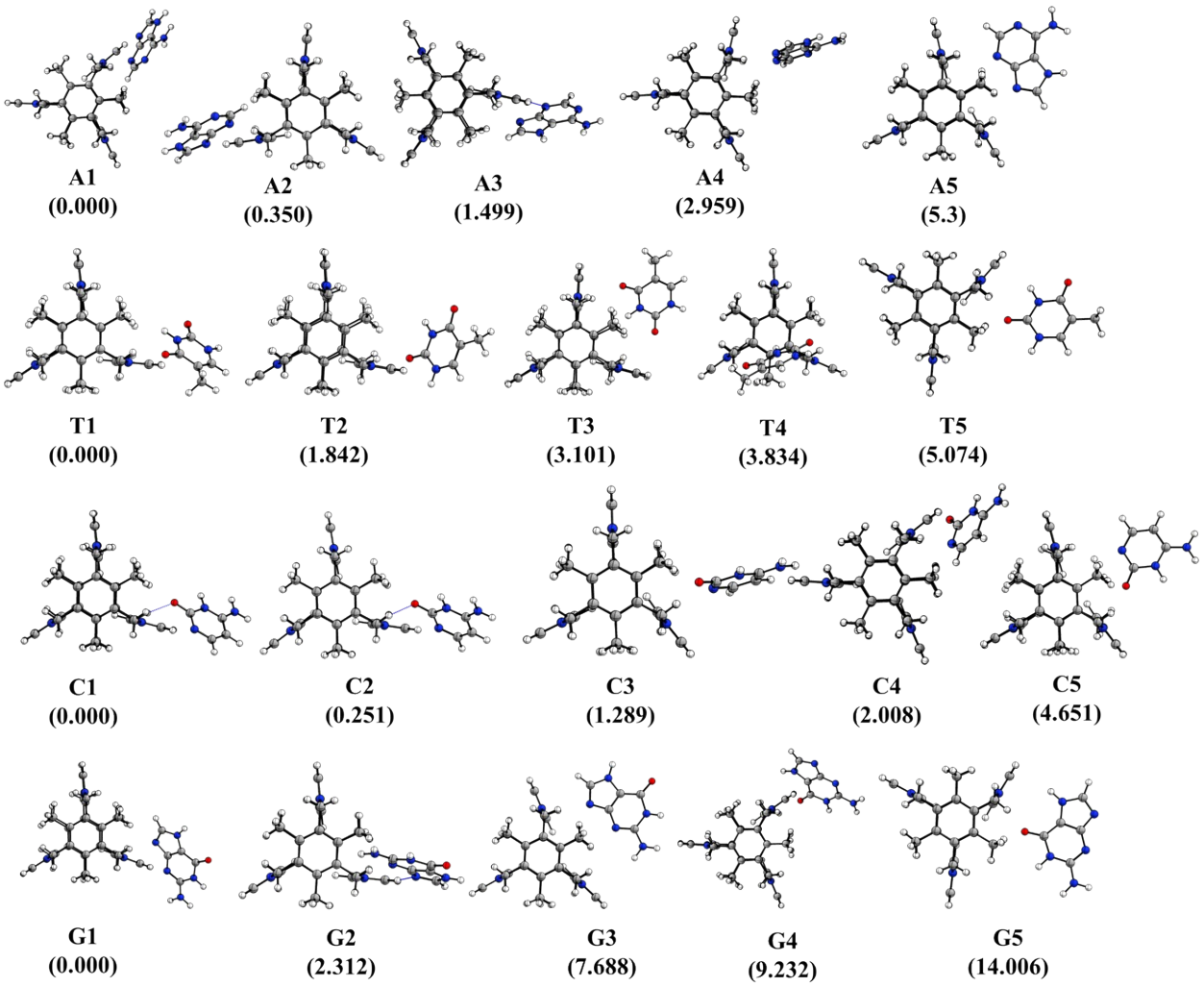

Figure S10. Optimized geometries of PC[1] complexes with DNA nucleobases-adenine (A), thymine (T), cytosine (C), and guanine (G), computed at the DFT level. The relative energies are in parentheses, expressed in kcal.mol^{-1}

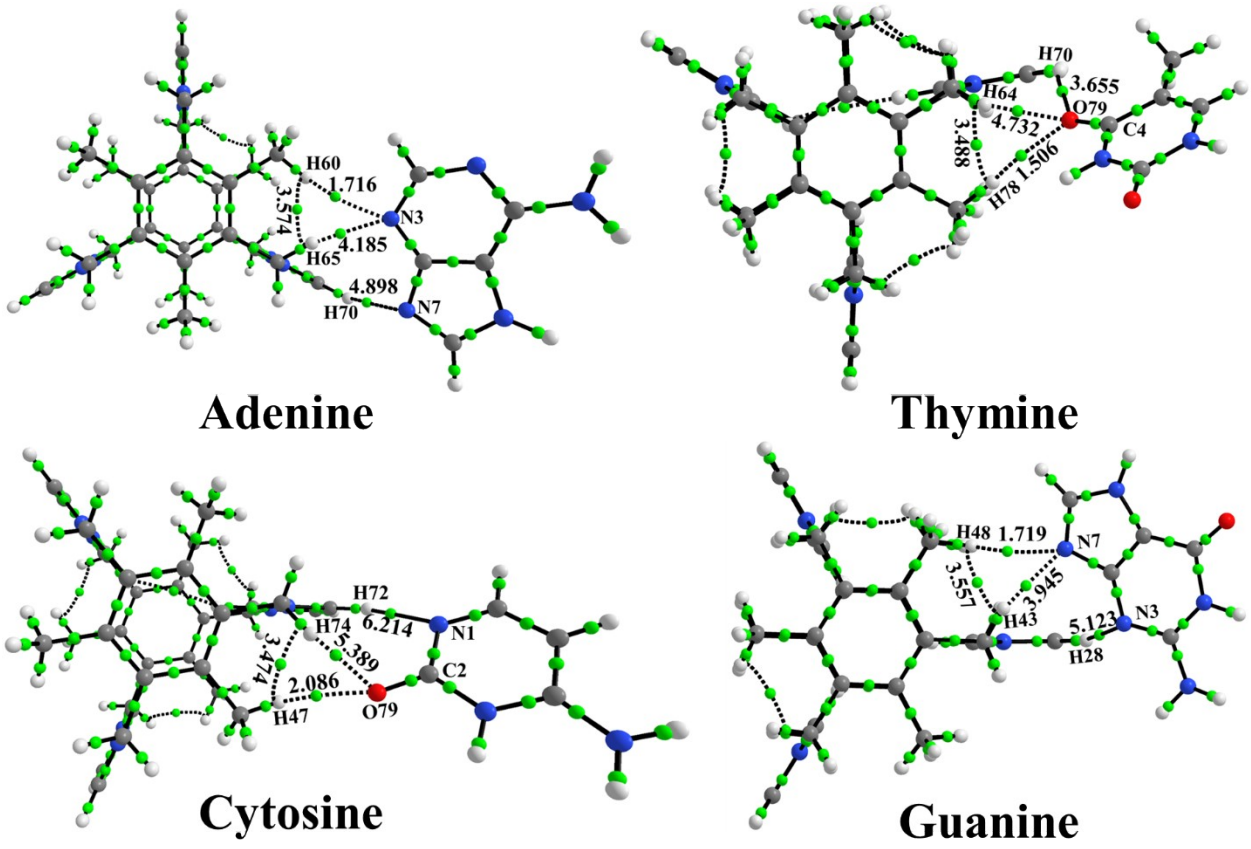

Figure S11. QTAIM-based BCP and bond path analysis of the PC[1]@nucleobase complexes. The BCPs correspond to the hydrogen bonds between PC[1] and the nucleobases, and their respective bond strengths in kcal.mol^{-1} were estimated using the Espinosa-Molins-Lecomte (EML) equation (half the value of potential energy density, i.e., ½*V(r)).

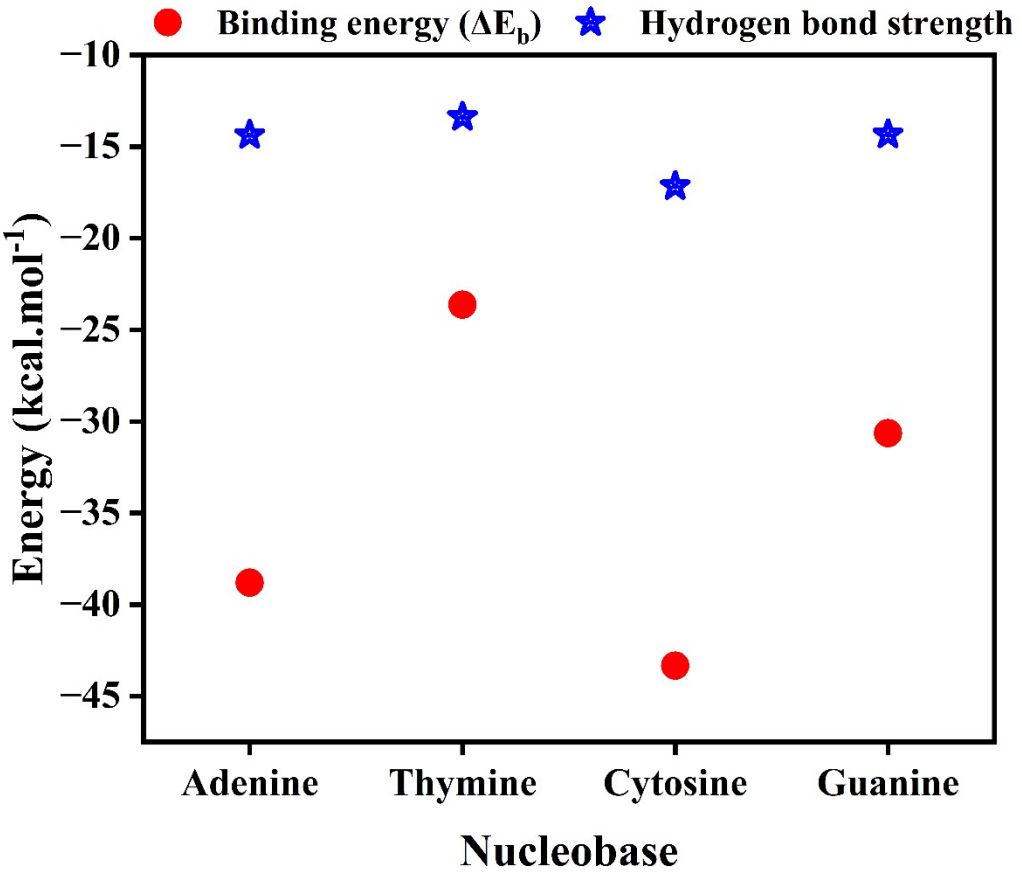

Figure S12. Comparison of binding energies (red curve) obtained from fully geometry-optimized PC[1]@nucleobase complexes (Table 1) and hydrogen-bond strengths (blue curve) evaluated using the EML semi-empirical model for adenine, thymine, cytosine, and guanine.

Table S15. QTAIM topological parameters for the noncovalent interactions between PC[1] and nucleobases (adenine, thymine, cytosine, and guanine). Listed are the electron density ρ(r), Laplacian $\nabla^2\rho$, Hessian eigenvalues (λ_1, λ_2, λ_3), potential energy density V(**r**), kinetic energy density G(**r**), total energy density K(**r**), (K(**r**)=V(**r**)+G(**r**)), and ellipticity ε at the corresponding bond critical points. All parameters are expressed in a.u.

Systems	ρ(r)	$\nabla^2\rho(r)$	λ_1	λ_2	λ_3	V(r)	G(r)	K(r)	ε
PC1@Adenine									
H60···H3	0.0169	0.0599	-0.0166	-0.0081	0.0845	-0.0114	0.0132	-0.0018	1.0474
H60···N3	0.0102	0.0331	-0.0089	-0.0056	0.0476	-0.0055	0.0069	-0.0014	0.5921
H65···N3	0.0212	0.0585	-0.0247	-0.0240	0.1071	-0.0133	0.0140	-0.0006	0.0300
H70···N7	0.0234	0.0653	-0.0294	-0.0286	0.1233	-0.0156	0.0160	-0.0004	0.0264
PC1@Thymine									
H64···H78	0.0166	0.0582	-0.0163	-0.0079	0.0824	-0.0111	0.0128	-0.0017	1.0611
H70···O=C4	0.0171	0.0658	-0.0196	-0.0180	0.1034	-0.0117	0.0141	-0.0024	0.0928
H64···O=C4	0.0202	0.0763	-0.0247	-0.0235	0.1245	-0.0151	0.0171	-0.0020	0.0548
H78···O=C4	0.0086	0.0324	-0.0079	-0.0048	0.0451	-0.0048	0.0065	-0.0017	0.6403
PC1@Cytosine									
H47···H74	0.0161	0.0585	-0.0149	-0.0060	0.0794	-0.0111	0.0129	-0.0018	1.4846
H74···O=C2	0.0232	0.0772	-0.0298	-0.0290	0.1360	-0.0172	0.0182	-0.0011	0.0261
H72···N1	0.0283	0.0704	-0.0380	-0.0366	0.1449	-0.0198	0.0187	0.0011	0.0375
H47···O=C4	0.0105	0.0443	-0.0099	-0.0078	0.0620	-0.0067	0.0089	-0.0022	0.2740
PC1@Guanine									
H43···H48	0.0169	0.0596	-0.0166	-0.0081	0.0844	-0.0113	0.0131	-0.0018	1.0553
H48···N7	0.0103	0.0330	-0.0093	-0.0065	0.0488	-0.0055	0.0069	-0.0014	0.4301
H43···N7	0.0202	0.0578	-0.0231	-0.0225	0.1034	-0.0126	0.0135	-0.0009	0.0282
H28···N3	0.0242	0.0656	-0.0305	-0.0294	0.1255	-0.0163	0.0164	0.0000	0.0371

Table S16. Energy decomposition analysis (EDA) of the PC[1]@nucleobase complexes showing the contribution of electrostatic (E_{elec}), dispersion (E_{disp}), induction (E_{ind}), and exchange (E_{exc}) components to the total interaction energy (E_{total}) in kcal.mol^{-1}. The values in parentheses represent the percentage contribution of each attractive component to the overall stabilization energy. DFT-D3 corrected interaction energies are also provided for comparison.

Energy components	Adenine	Thymine	Cytosine	Guanine
Electrostatic (E_{elec})	-36.836 (61.562)	-23.658 (58.934)	-46.339 (66.855)	-28.750 (55.478)
Dispersion (E_{disp})	-13.528 (15.830)	-10.342 (15.303)	-15.010 (11.490)	-13.585 (18.307)
Induction (E_{ind})	-9.472 (22.608)	-6.143 (25.763)	-7.964 (21.655)	-9.487 (26.215)
Exchange (E_{exc})	20.454	13.488	22.509	20.468
Total energy (E_{total})	-39.382	-26.656	-46.804	-31.353
DFT-D3	-38.796	-23.632	-43.326	-30.645

Table S17. Natural Bond Orbital (NBO) analysis of the PC[1]@nucleobase complexes showing donor–acceptor interactions, where the nucleobase acts as the donor and PC[1] as the acceptor. The corresponding second-order perturbation stabilization energies, E(2) (in kcal·mol^{-1}), represent the strength of charge transfer and delocalization interactions contributing to complex stability.

Donor	Acceptor	E(2) in kcal.mol^{-1}
Adenine		
LP (1) N7	C69 - H70	8.13
LP (1) N3	C58 - H60	0.86
LP (1) N3	C63 - H65	5.58
Thymine		
LP (1) O=C4	C63 - H64	2.77
LP (1) O=C4	C66 - H78	0.33
LP (1) O=C4	C69 - H70	1.18
LP (2) O=C4	C63 - H64	1.11
LP (2) O=C4	C66 - H78	0.37
LP (2) O=C4	C69 - H70	2.05
Cytosine		
LP (1) O=C2	C45 - H47	0.58
LP (1) O=C2	C73 - H74	2.18
LP (2) O=C2	C45 - H47	0.27
LP (2) O=C2	C73 - H74	3.44
LP (1) N1	C71 - H72	12.31
Guanine		
LP (1) N3	C27 - H28	8.03
LP (1) N7	C42 - H43	5.14
LP (1) N7	C45 - H48	1.03

References

1 S. Grimme, A. Hansen, J. G. Brandenburg and C. Bannwarth, *Chem. Rev.*, 2016, **116**, 5105–5154.

2 J. L. Bao, L. Gagliardi and D. G. Truhlar, *J. Phys. Chem. Lett.*, 2018, **9**, 2353–2358.

3 R. Peverati and D. G. Truhlar, *J. Chem. Theory Comput.*, 2012, **8**, 2310–2319.

4 B. Kanungo, J. Hatch, P. M. Zimmerman and V. Gavini, *Sci. Adv.*, 2025, **11**, eady8962.

5 Y. Zhao and D. G. Truhlar, *Acc. Chem. Res.*, 2008, **41**, 157–167.

6 S. Jana and P. Samal, *Physical Chemistry Chemical Physics*, 2018, **20**, 8999–9005.

7 N. Mardirossian and M. Head-Gordon, *Molecular Physics*, 2017, **115**, 2315–2372.

8 S. F. Boys and F. Bernardi, *Molecular Physics*, 1970, **19**, 553–566.

9 M. S. Brozzo, S. Bjelić, K. Kisko, T. Schleier, V.-M. Leppänen, K. Alitalo, F. K. Winkler and K. Ballmer-Hofer, *Blood, The Journal of the American Society of Hematology*, 2012, **119**, 1781–1788.

10 V.-M. Leppänen, A. E. Prota, M. Jeltsch, A. Anisimov, N. Kalkkinen, T. Strandin, H. Lankinen, A. Goldman, K. Ballmer-Hofer and K. Alitalo, *Proc. Natl. Acad. Sci. U.S.A.*, 2010, **107**, 2425–2430.

11 J. Dapkūnas, A. Timinskas, K. Olechnovič, M. Tomkuvienė and Č. Venclovas, *Nucleic Acids Research*, 2024, **52**, W264–W271.

12 O. Trott and A. J. Olson, *J Comput Chem*, 2010, **31**, 455–461.

13 D. A. Case, H. M. Aktulga, K. Belfon, D. S. Cerutti, G. A. Cisneros, V. W. D. Cruzeiro, N. Forouzesh, T. J. Giese, A. W. Götz, H. Gohlke, S. Izadi, K. Kasavajhala, M. C. Kaymak, E. King, T. Kurtzman, T.-S. Lee, P. Li, J. Liu, T. Luchko, R. Luo, M. Manathunga, M. R. Machado, H. M. Nguyen, K. A. O'Hearn, A. V. Onufriev, F. Pan, S. Pantano, R. Qi, A. Rahnamoun, A. Risheh, S. Schott-Verdugo, A. Shajan, J. Swails, J. Wang, H. Wei, X. Wu, Y. Wu, S. Zhang, S. Zhao, Q. Zhu, T. E. Cheatham, D. R. Roe, A. Roitberg, C. Simmerling, D. M. York, M. C. Nagan and K. M. Merz, *J. Chem. Inf. Model.*, 2023, **63**, 6183–6191.

14 W. Zhu, Y. Wang, K. Li, J. Gao, C.-H. Huang, C.-C. Chen, T.-P. Ko, Y. Zhang, R.-T. Guo and E. Oldfield, *J. Med. Chem.*, 2015, **58**, 1215–1227.

15 D. R. Boer, J. M. C. A. Kerckhoffs, Y. Parajo, M. Pascu, I. Usón, P. Lincoln, M. J. Hannon and M. Coll, *Angew Chem Int Ed*, 2010, **49**, 2336–2339.

16 W. D. Cornell, P. Cieplak, C. I. Bayly and P. A. Kollman, *J. Am. Chem. Soc.*, 1993, **115**, 9620–9631.

17 M. J. Frisch, G. W. Trucks, H. B. Schlegel, G. E. Scuseria, M. A. Robb, J. R. Cheeseman, G. Scalmani, V. Barone, G. A. Petersson and H. Nakatsuji, *There is no corresponding record for this reference*.

18 C. Tian, K. Kasavajhala, K. A. A. Belfon, L. Raguette, H. Huang, A. N. Migues, J. Bickel, Y. Wang, J. Pincay, Q. Wu and C. Simmerling, *J. Chem. Theory Comput.*, 2020, **16**, 528–552.

19 R. Galindo-Murillo, J. C. Robertson, M. Zgarbová, J. Šponer, M. Otyepka, P. Jurečka and T. E. Cheatham, *J. Chem. Theory Comput.*, 2016, **12**, 4114–4127.

20 F. Fogolari, A. Brigo and H. Molinari, *Biophysical Journal*, 2003, **85**, 159–166.

21 E. Wang, H. Sun, J. Wang, Z. Wang, H. Liu, J. Z. H. Zhang and T. Hou, *Chem. Rev.*, 2019, **119**, 9478–9508.

22 S. I. Virtanen, S. P. Niinivehmas and O. T. Pentikäinen, *Journal of Molecular Graphics and Modelling*, 2015, **62**, 303–318.

23 C. R. W. Guimarães and M. Cardozo, *J. Chem. Inf. Model.*, 2008, **48**, 958–970.

24 M. K. Gilson and B. Honig, *Proteins*, 1988, **4**, 7–18.

25 J. Wang, T. Hou and X. Xu, *CAD*, 2006, **2**, 287–306.

26 P. A. Kollman, I. Massova, C. Reyes, B. Kuhn, S. Huo, L. Chong, M. Lee, T. Lee, Y. Duan, W. Wang, O. Donini, P. Cieplak, J. Srinivasan, D. A. Case and T. E. Cheatham, *Acc. Chem. Res.*, 2000, **33**, 889–897.

27 A. Lindström, L. Edvinsson, A. Johansson, C. D. Andersson, I. E. Andersson, F. Raubacher and A. Linusson, *J. Chem. Inf. Model.*, 2011, **51**, 267–282.

28 T. Hou, J. Wang, Y. Li and W. Wang, *J. Chem. Inf. Model.*, 2011, **51**, 69–82.

29 T. Lu and F. Chen, *Journal of computational chemistry*, 2012, **33**, 580–592.

30 J. Černỳ and P. Hobza, *Physical Chemistry Chemical Physics*, 2007, **9**, 5291–5303.

31 T. A. Keith, *TK Gristmill Software: Overland Park, KS, USA*.

32 J. M. Turney, A. C. Simmonett, R. M. Parrish, E. G. Hohenstein, F. A. Evangelista, J. T. Fermann, B. J. Mintz, L. A. Burns, J. J. Wilke, M. L. Abrams, N. J. Russ, M. L. Leininger, C. L. Janssen, E. T. Seidl, W. D. Allen, H. F. Schaefer, R. A. King, E. F. Valeev, C. D. Sherrill and T. D. Crawford, *WIREs Comput Mol Sci*, 2012, **2**, 556–565.

33 R. M. Parrish and C. D. Sherrill, *The Journal of chemical physics*.

34 G. A. Andrienko, *See https://www. chemcraftprog. com*.

35 J. P. Foster and F. Weinhold, *J. Am. Chem. Soc.*, 1980, **102**, 7211–7218.

36 A. E. Reed, L. A. Curtiss and F. Weinhold, *Chem. Rev.*, 1988, **88**, 899–926.

Coordinates

All the coordinates are supplied here is at the level of B3PW91-D3/def2TZVPP level of theory

PC[2]

N	-1.477692000000	-1.217314000000	-3.175492000000
N	-3.646214000000	-1.221569000000	-3.180353000000
N	-1.477088000000	-2.143474000000	2.640727000000
N	1.475221000000	-3.359321000000	-0.533770000000
N	-3.645615000000	-2.145013000000	2.647931000000
N	3.643777000000	-3.366875000000	-0.532866000000
C	-0.004753000000	-0.499672000000	-1.315844000000
C	0.003480000000	-1.389279000000	-0.225167000000
C	-0.004650000000	-0.889681000000	1.090645000000
C	-5.074647000000	-0.878925000000	1.086048000000
C	-3.240960000000	-1.706858000000	-4.403532000000
H	-3.938392000000	-2.011858000000	-5.169540000000
C	-1.880586000000	-1.706118000000	-4.405669000000
H	-1.186284000000	-2.010068000000	-5.173270000000
C	-5.064262000000	0.890666000000	-1.095976000000
C	-5.064422000000	-1.392897000000	-0.220938000000
C	-0.083584000000	-1.038656000000	-2.734558000000
H	0.412582000000	-0.377260000000	-3.442693000000
H	0.424460000000	-1.997039000000	-2.827242000000
C	-5.063804000000	0.506601000000	1.319141000000
C	-2.572332000000	-0.933303000000	-2.458531000000
H	-2.599492000000	-0.537250000000	-1.462576000000

C	2.570336000000	-2.597229000000	-0.419938000000
H	2.598211000000	-1.537016000000	-0.262726000000
C	0.081340000000	-2.887442000000	-0.467716000000
H	-0.427051000000	-3.446590000000	0.315932000000
H	-0.415040000000	-3.169665000000	-1.394550000000
C	-2.571903000000	-1.659822000000	2.040409000000
H	-2.599437000000	-0.988659000000	1.204767000000
C	-5.073941000000	1.381451000000	0.220484000000
C	-3.240053000000	-2.969366000000	3.673530000000
H	-3.937296000000	-3.484774000000	4.317280000000
C	-5.075030000000	-0.498225000000	-1.304210000000
C	-0.083064000000	-1.849085000000	2.266597000000
H	0.414106000000	-2.792442000000	2.047583000000
H	0.424193000000	-1.450122000000	3.143373000000
C	-1.879672000000	-2.971938000000	3.673279000000
H	-1.185174000000	-3.489735000000	4.316093000000
C	1.877363000000	-4.668894000000	-0.728256000000
H	1.182573000000	-5.484981000000	-0.850393000000
C	-5.050345000000	-1.039160000000	-2.712259000000
H	-5.543469000000	-2.005299000000	-2.795988000000
H	-5.541798000000	-0.377410000000	-3.422283000000
C	3.237740000000	-4.668186000000	-0.726745000000
H	3.934691000000	-5.484221000000	-0.847392000000
C	-5.047752000000	1.839794000000	-2.264054000000
H	-6.067649000000	2.100604000000	-2.564464000000
H	-4.557808000000	1.423876000000	-3.142333000000
H	-4.535550000000	2.774479000000	-2.043018000000
C	5.048245000000	-2.871272000000	-0.456364000000
H	5.539585000000	-3.155293000000	-1.384526000000
H	5.541007000000	-3.427462000000	0.338264000000
C	-5.049810000000	-1.828148000000	2.258334000000
H	-5.541094000000	-1.417179000000	3.137733000000
H	-5.543125000000	-2.773023000000	2.040628000000
C	-5.046715000000	1.043644000000	2.725115000000
H	-6.066439000000	1.174351000000	3.101324000000
H	-4.555782000000	2.011711000000	2.803916000000
H	-4.535111000000	0.384356000000	3.424018000000
C	-5.046944000000	-2.878895000000	-0.459682000000
H	-4.561281000000	-3.432174000000	0.341709000000
H	-4.529720000000	-3.153884000000	-1.377226000000
H	-6.066429000000	-3.269369000000	-0.541159000000
N	1.477693000000	1.217302000000	3.175494000000
N	3.646215000000	1.221553000000	3.180355000000

N	1.477088000000	2.143486000000	-2.640723000000
N	-1.475222000000	3.359322000000	0.533773000000
N	3.645615000000	2.145025000000	-2.647927000000
N	-3.643777000000	3.366876000000	0.532861000000
C	0.004753000000	0.499675000000	1.315841000000
C	-0.003480000000	1.389281000000	0.225164000000
C	0.004650000000	0.889684000000	-1.090649000000
C	5.074646000000	0.878928000000	-1.086051000000
C	3.240961000000	1.706815000000	4.403545000000
H	3.938394000000	2.011797000000	5.169560000000
C	1.880587000000	1.706079000000	4.405681000000
H	1.186286000000	2.010014000000	5.173288000000
C	5.064262000000	-0.890667000000	1.095969000000
C	5.064422000000	1.392897000000	0.220937000000
C	0.083584000000	1.038658000000	2.734555000000
H	-0.412590000000	0.377266000000	3.442688000000
H	-0.424450000000	1.997046000000	2.827237000000
C	5.063804000000	-0.506598000000	-1.319146000000
C	2.572333000000	0.933306000000	2.458526000000
H	2.599492000000	0.537275000000	1.462563000000
C	-2.570337000000	2.597231000000	0.419932000000
H	-2.598211000000	1.537019000000	0.262718000000
C	-0.081340000000	2.887445000000	0.467713000000
H	0.427047000000	3.446592000000	-0.315937000000
H	0.415043000000	3.169668000000	1.394546000000
C	2.571903000000	1.659823000000	-2.040413000000
H	2.599437000000	0.988647000000	-1.204782000000
C	5.073941000000	-1.381450000000	-0.220491000000
C	3.240053000000	2.969395000000	-3.673511000000
H	3.937297000000	3.484814000000	-4.317253000000
C	5.075030000000	0.498223000000	1.304207000000
C	0.083064000000	1.849088000000	-2.266600000000
H	-0.414112000000	2.792442000000	-2.047588000000
H	-0.424187000000	1.450123000000	-3.143378000000
C	1.879672000000	2.971966000000	-3.673262000000
H	1.185174000000	3.489773000000	-4.316068000000
C	-1.877364000000	4.668894000000	0.728265000000
H	-1.182575000000	5.484980000000	0.850409000000
C	5.050345000000	1.039150000000	2.712258000000
H	5.543468000000	2.005289000000	2.795993000000
H	5.541800000000	0.377396000000	3.422278000000
C	-3.237742000000	4.668186000000	0.726749000000
H	-3.934692000000	5.484221000000	0.847397000000

C	5.047755000000	-1.839793000000	2.264049000000
H	6.067652000000	-2.100585000000	2.564472000000
H	4.557793000000	-1.423880000000	3.142321000000
H	4.535570000000	-2.774488000000	2.043011000000
C	-5.048246000000	2.871275000000	0.456349000000
H	-5.539594000000	3.155302000000	1.384504000000
H	-5.540999000000	3.427460000000	-0.338287000000
C	5.049809000000	1.828158000000	-2.258332000000
H	5.541095000000	1.417196000000	-3.137732000000
H	5.543124000000	2.773032000000	-2.040618000000
C	5.046714000000	-1.043645000000	-2.725119000000
H	6.066439000000	-1.174396000000	-3.101312000000
H	4.555744000000	-2.011693000000	-2.803919000000
H	4.535147000000	-0.384342000000	-3.424034000000
C	5.046942000000	2.878896000000	0.459679000000
H	4.561261000000	3.432169000000	-0.341705000000
H	4.529735000000	3.153886000000	1.377231000000
H	6.066427000000	3.269374000000	0.541134000000

PC[1]

N	3.014996000000	-1.601656000000	-1.081559000000
N	3.015389000000	-1.599854000000	1.083356000000
N	-0.120537000000	3.410409000000	-1.084614000000
N	-0.120989000000	3.411683000000	1.080307000000
C	1.233336000000	-0.655988000000	-2.496009000000
C	1.194131000000	0.746141000000	-2.479979000000
C	-0.050372000000	1.393661000000	-2.497333000000
C	-0.050716000000	1.396652000000	2.495643000000
C	4.176485000000	-2.222280000000	0.681355000000
H	4.898522000000	-2.608687000000	1.381488000000
C	4.176268000000	-2.223357000000	-0.678948000000
H	4.898076000000	-2.610881000000	-1.378701000000
C	0.051249000000	-1.406911000000	2.480081000000
C	1.194058000000	0.749796000000	2.479155000000
C	2.566110000000	-1.363081000000	-2.471703000000
H	2.521943000000	-2.328202000000	-2.971737000000
H	3.340614000000	-0.785546000000	-2.971735000000
C	-1.245126000000	0.661058000000	2.479348000000
C	2.335648000000	-1.236495000000	0.000712000000
H	1.391346000000	-0.730488000000	0.000457000000
C	2.469347000000	1.543989000000	-2.419429000000
H	2.343060000000	2.493127000000	-1.902548000000
H	2.840472000000	1.768999000000	-3.423324000000

C	-0.097937000000	2.640316000000	-0.001682000000
H	-0.066124000000	1.569393000000	-0.000983000000
C	-1.183041000000	-0.740394000000	2.496755000000
C	-0.160188000000	4.728167000000	0.677212000000
H	-0.184586000000	5.547316000000	1.376666000000
C	1.233872000000	-0.652349000000	2.496656000000
C	-0.104114000000	2.901410000000	-2.474362000000
H	0.753394000000	3.345085000000	-2.975591000000
H	-0.991724000000	3.283180000000	-2.974139000000
C	-0.159956000000	4.727365000000	-0.683064000000
H	-0.184064000000	5.545697000000	-1.383482000000
C	2.566871000000	-1.359050000000	2.473229000000
H	3.341310000000	-0.780466000000	2.972115000000
H	2.523161000000	-2.323289000000	2.974997000000
C	0.106561000000	-2.910173000000	2.419741000000
H	0.125626000000	-3.343666000000	3.423671000000
H	0.987999000000	-3.273531000000	1.895151000000
H	-0.748560000000	-3.338112000000	1.900412000000
C	-0.105459000000	2.904335000000	2.470694000000
H	-0.993963000000	3.286051000000	2.968958000000
H	0.751287000000	3.349299000000	2.972109000000
C	-2.574050000000	1.365848000000	2.418800000000
H	-2.954625000000	1.574286000000	3.422732000000
H	-3.332578000000	0.781681000000	1.901748000000
H	-2.517489000000	2.316398000000	1.892023000000
C	2.468433000000	1.548944000000	2.418121000000
H	2.342324000000	2.494526000000	1.894593000000
H	3.265805000000	1.022448000000	1.897457000000
H	2.835443000000	1.781086000000	3.421901000000
N	-2.894832000000	-1.810284000000	-1.081249000000
N	-2.894546000000	-1.809330000000	1.083688000000
C	-1.244967000000	0.658444000000	-2.479968000000
C	-1.183419000000	-0.743124000000	-2.495924000000
C	0.050474000000	-1.410172000000	-2.478816000000
C	-2.574708000000	1.361787000000	-2.419805000000
H	-2.516494000000	2.321726000000	-1.910926000000
H	-3.326558000000	0.784607000000	-1.885077000000
C	-2.237971000000	-1.405836000000	0.000947000000
H	-1.325649000000	-0.844190000000	0.000569000000
C	-2.462611000000	-1.543064000000	-2.471465000000
H	-2.350070000000	-2.503222000000	-2.970281000000
H	-3.275652000000	-1.022331000000	-2.972706000000
C	0.105895000000	-2.913332000000	-2.417015000000

H	0.983973000000	-3.275610000000	-1.885951000000
H	0.132311000000	-3.347464000000	-3.420503000000
C	-4.016476000000	-2.500842000000	-0.678464000000
H	-4.714192000000	-2.930403000000	-1.378114000000
C	-4.016319000000	-2.500202000000	0.681826000000
H	-4.713807000000	-2.929199000000	1.382048000000
C	-2.461475000000	-1.541570000000	2.473510000000
H	-3.274619000000	-1.021827000000	2.975583000000
H	-2.347415000000	-2.501598000000	2.972239000000
H	3.263830000000	1.019396000000	-1.892331000000
H	-2.965179000000	1.551041000000	-3.423740000000
H	-0.752509000000	-3.341548000000	-1.903485000000

PC[1]@Adenine

N	-3.413987000000	-1.884726000000	2.430941000000
N	-4.494815000000	-2.058386000000	0.563654000000
N	-1.496608000000	3.464845000000	0.840811000000
N	-2.593959000000	3.300103000000	-1.017251000000
C	-1.327814000000	-0.612272000000	2.748336000000
C	-1.511550000000	0.778350000000	2.712231000000
C	-0.537117000000	1.573557000000	2.095707000000
C	-3.058121000000	1.194807000000	-2.206313000000
C	-5.197044000000	-2.779722000000	1.503427000000
H	-6.107935000000	-3.304195000000	1.267586000000
C	-4.517830000000	-2.670309000000	2.676635000000
H	-4.729522000000	-3.081925000000	3.649331000000
C	-2.702677000000	-1.586401000000	-2.151895000000
C	-4.007847000000	0.388861000000	-1.560494000000
C	-2.372799000000	-1.479739000000	3.403132000000
H	-1.943460000000	-2.388820000000	3.818543000000
H	-2.874391000000	-0.965193000000	4.219921000000
C	-1.920496000000	0.630971000000	-2.801164000000
C	-3.424905000000	-1.530864000000	1.150361000000
H	-2.688335000000	-0.918917000000	0.669386000000
C	-2.749874000000	1.396275000000	3.306142000000
H	-3.010009000000	2.344451000000	2.840995000000
H	-2.622817000000	1.585647000000	4.375646000000
C	-1.937883000000	2.618612000000	-0.083062000000
H	-1.785637000000	1.557833000000	-0.075899000000
C	-1.765918000000	-0.763063000000	-2.791389000000
C	-2.571446000000	4.635228000000	-0.680615000000
H	-3.040754000000	5.392243000000	-1.286452000000
C	-3.833490000000	-1.002185000000	-1.560833000000

C	-0.718335000000	3.069031000000	2.036538000000
H	-1.245119000000	3.451935000000	2.908002000000
H	0.235913000000	3.588647000000	1.987439000000
C	-1.881161000000	4.738470000000	0.486646000000
H	-1.638497000000	5.602278000000	1.082674000000
C	-4.842704000000	-1.879496000000	-0.863496000000
H	-5.844569000000	-1.457657000000	-0.905558000000
H	-4.898618000000	-2.868285000000	-1.313463000000
C	-2.482458000000	-3.073547000000	-2.072201000000
H	-2.944269000000	-3.586199000000	-2.920641000000
H	-2.900534000000	-3.507551000000	-1.165829000000
H	-1.426849000000	-3.336482000000	-2.071035000000
C	-3.234494000000	2.692427000000	-2.204280000000
H	-2.796195000000	3.153398000000	-3.086713000000
H	-4.284539000000	2.976341000000	-2.190004000000
C	-0.857165000000	1.501960000000	-3.415155000000
H	-1.005364000000	1.603229000000	-4.493865000000
H	0.141923000000	1.097432000000	-3.260743000000
H	-0.842046000000	2.505700000000	-2.997011000000
C	-5.181420000000	1.015211000000	-0.854894000000
H	-4.937170000000	1.986494000000	-0.428224000000
H	-5.544650000000	0.408871000000	-0.028022000000
H	-6.020528000000	1.163473000000	-1.540375000000
N	1.635686000000	-1.327641000000	-0.564510000000
N	0.559834000000	-1.474386000000	-2.434669000000
C	0.586532000000	0.997177000000	1.480821000000
C	0.750936000000	-0.394312000000	1.523966000000
C	-0.216621000000	-1.208199000000	2.134774000000
C	1.574331000000	1.873613000000	0.760808000000
H	1.074146000000	2.613931000000	0.134039000000
H	2.255556000000	1.317096000000	0.122457000000
C	0.470468000000	-1.102673000000	-1.159581000000
H	-0.399834000000	-0.688624000000	-0.692512000000
C	1.940462000000	-1.026407000000	0.848299000000
H	2.238205000000	-1.958032000000	1.323485000000
H	2.825843000000	-0.384744000000	0.834934000000
C	-0.072487000000	-2.706546000000	2.103753000000
H	-1.031001000000	-3.220899000000	2.132465000000
H	0.513096000000	-3.062780000000	2.955766000000
C	2.511847000000	-1.859694000000	-1.482179000000
H	3.532784000000	-2.096726000000	-1.193027000000
C	1.833020000000	-1.954216000000	-2.658226000000
H	2.148464000000	-2.313753000000	-3.622876000000

C	-0.536377000000	-1.375120000000	-3.415874000000
H	-0.176816000000	-0.784254000000	-4.255753000000
H	-0.734027000000	-2.374270000000	-3.798715000000
H	-3.624908000000	0.757821000000	3.193122000000
H	2.198304000000	2.418503000000	1.474334000000
H	0.430471000000	-3.051635000000	1.202715000000
N	7.485922000000	-1.567164000000	0.106810000000
N	5.290168000000	-1.872163000000	-0.095012000000
N	4.635294000000	0.457478000000	0.001431000000
N	6.467219000000	1.980937000000	0.234281000000
N	8.673775000000	1.364558000000	0.381110000000
C	6.921340000000	-0.310566000000	0.138379000000
C	5.549337000000	-0.528015000000	0.012554000000
C	7.388719000000	1.011065000000	0.253716000000
C	6.469412000000	-2.449144000000	-0.034361000000
C	5.185581000000	1.662008000000	0.114517000000
H	8.459726000000	-1.811490000000	0.173167000000
H	6.645402000000	-3.512851000000	-0.089711000000
H	4.503915000000	2.507743000000	0.106953000000
H	8.896240000000	2.343746000000	0.447695000000
H	9.426980000000	0.703488000000	0.394216000000

PC[1]@Thymine

N	1.139686000000	3.255516000000	-1.342525000000
N	2.359928000000	2.153325000000	-2.749097000000
N	3.467748000000	0.094109000000	3.057506000000
N	4.640258000000	-1.052969000000	1.645075000000
C	0.277722000000	2.380940000000	0.793620000000
C	1.307107000000	2.212727000000	1.729862000000
C	1.268605000000	1.104438000000	2.588268000000
C	4.002056000000	-1.506661000000	-0.689961000000
C	2.255266000000	3.439526000000	-3.229339000000
H	2.729343000000	3.755809000000	-4.143499000000
C	1.487738000000	4.131725000000	-2.345682000000
H	1.169939000000	5.161013000000	-2.350247000000
C	2.016540000000	-1.106030000000	-2.628026000000
C	4.051944000000	-0.368219000000	-1.503720000000
C	0.315542000000	3.556174000000	-0.150198000000
H	-0.676741000000	3.825961000000	-0.503165000000
H	0.738798000000	4.442204000000	0.318576000000
C	2.957466000000	-2.439112000000	-0.814045000000
C	1.675280000000	2.069672000000	-1.611912000000
H	1.569274000000	1.188536000000	-1.010081000000

C	2.448898000000	3.191974000000	1.803904000000
H	3.389251000000	2.711392000000	2.070077000000
H	2.256925000000	3.965314000000	2.552916000000
C	3.528655000000	-0.341148000000	1.803438000000
H	2.799226000000	-0.146428000000	1.042685000000
C	1.982458000000	-2.239836000000	-1.799276000000
C	5.320394000000	-1.072835000000	2.842322000000
H	6.256694000000	-1.590845000000	2.967131000000
C	3.066600000000	-0.190604000000	-2.488888000000
C	2.365476000000	0.916272000000	3.606270000000
H	2.791772000000	1.865066000000	3.924538000000
H	2.003933000000	0.416991000000	4.502669000000
C	4.583703000000	-0.351711000000	3.729617000000
H	4.761903000000	-0.126618000000	4.767948000000
C	3.113389000000	1.037722000000	-3.362100000000
H	4.132867000000	1.383266000000	-3.518633000000
H	2.690307000000	0.853803000000	-4.347142000000
C	0.913762000000	-0.881001000000	-3.627340000000
H	1.065929000000	-1.489520000000	-4.523133000000
H	0.838832000000	0.152999000000	-3.953164000000
H	-0.062824000000	-1.140152000000	-3.219990000000
C	5.045161000000	-1.707300000000	0.380823000000
H	5.204852000000	-2.761156000000	0.597590000000
H	6.009966000000	-1.296451000000	0.091396000000
C	2.883529000000	-3.610855000000	0.128899000000
H	3.528430000000	-4.428035000000	-0.205648000000
H	1.878642000000	-4.015233000000	0.221997000000
H	3.195259000000	-3.344164000000	1.138241000000
C	5.124002000000	0.672370000000	-1.316788000000
H	5.556255000000	0.659700000000	-0.319336000000
H	4.744177000000	1.682385000000	-1.466035000000
H	5.944273000000	0.525319000000	-2.024880000000
N	-1.513701000000	-1.636903000000	0.269291000000
N	-0.338848000000	-2.741814000000	-1.172350000000
C	0.255037000000	0.140682000000	2.475383000000
C	-0.767046000000	0.327139000000	1.531177000000
C	-0.760273000000	1.442554000000	0.680385000000
C	0.276303000000	-1.092036000000	3.341101000000
H	1.277430000000	-1.354823000000	3.675210000000
H	-0.107082000000	-1.968015000000	2.820276000000
C	-0.281615000000	-1.867787000000	-0.171169000000
H	0.611865000000	-1.410698000000	0.205689000000
C	-1.846217000000	-0.715113000000	1.376188000000

H	-2.822414000000	-0.292834000000	1.141229000000
H	-1.974326000000	-1.310679000000	2.276678000000
C	-1.822039000000	1.633581000000	-0.369469000000
H	-1.381710000000	1.752433000000	-1.362448000000
H	-2.405667000000	2.535169000000	-0.168386000000
C	-2.397699000000	-2.391825000000	-0.466967000000
H	-3.462863000000	-2.302550000000	-0.312044000000
C	-1.657474000000	-3.089635000000	-1.371232000000
H	-1.958251000000	-3.782547000000	-2.138586000000
C	0.831549000000	-3.206227000000	-1.942371000000
H	1.089289000000	-4.207761000000	-1.605915000000
H	0.515538000000	-3.297933000000	-2.979239000000
H	2.629370000000	3.698830000000	0.858793000000
H	-0.338419000000	-0.956634000000	4.235141000000
H	-2.534956000000	0.816236000000	-0.429228000000
O	-4.601616000000	-0.487344000000	0.095887000000
O	-7.858119000000	2.593083000000	0.819351000000
N	-6.258345000000	1.009269000000	0.449772000000
N	-8.485072000000	0.472700000000	0.226377000000
C	-6.848535000000	-1.214895000000	-0.177472000000
C	-5.818310000000	-0.250566000000	0.120411000000
C	-8.135339000000	-0.797437000000	-0.106638000000
C	-6.454139000000	-2.607452000000	-0.542803000000
C	-7.571377000000	1.464319000000	0.525944000000
H	-8.961753000000	-1.465178000000	-0.315060000000
H	-5.563433000000	1.706245000000	0.670010000000
H	-9.454621000000	0.749409000000	0.269703000000
H	-7.326993000000	-3.226767000000	-0.743893000000
H	-5.826794000000	-2.613165000000	-1.437763000000
H	-5.889902000000	-3.079592000000	0.265484000000

PC[1]@Cytosine

N	4.197470000000	-2.235502000000	0.529291000000
N	3.177175000000	-1.965533000000	2.419022000000
N	2.596097000000	3.207307000000	-1.077680000000
N	1.546789000000	3.464390000000	0.797252000000
C	3.558249000000	-1.164121000000	-1.594358000000
C	3.813646000000	0.213172000000	-1.617979000000
C	2.896647000000	1.065393000000	-2.253245000000
C	0.493407000000	1.655061000000	2.095224000000
C	4.206411000000	-2.852720000000	2.640809000000
H	4.397452000000	-3.286249000000	3.608223000000
C	4.847533000000	-3.022772000000	1.453468000000

H	5.698473000000	-3.631718000000	1.197617000000
C	0.027330000000	-1.103720000000	2.189095000000
C	1.439964000000	0.818887000000	2.701869000000
C	4.527287000000	-2.092295000000	-0.906223000000
H	4.513340000000	-3.087888000000	-1.344264000000
H	5.551977000000	-1.733309000000	-0.973697000000
C	-0.674762000000	1.131771000000	1.517970000000
C	3.195804000000	-1.609316000000	1.139201000000
H	2.512386000000	-0.926283000000	0.675612000000
C	5.036478000000	0.783383000000	-0.949449000000
H	4.843248000000	1.756148000000	-0.499705000000
H	5.853461000000	0.912403000000	-1.664841000000
C	1.885935000000	2.586714000000	-0.140319000000
H	1.624492000000	1.547092000000	-0.140370000000
C	-0.910385000000	-0.249283000000	1.588549000000
C	2.052579000000	4.695968000000	0.447477000000
H	1.907643000000	5.573731000000	1.054686000000
C	1.183928000000	-0.558437000000	2.766497000000
C	3.162726000000	2.549356000000	-2.275086000000
H	4.228148000000	2.768378000000	-2.292025000000
H	2.729745000000	3.026954000000	-3.151245000000
C	2.712828000000	4.534697000000	-0.730417000000
H	3.249191000000	5.245635000000	-1.336345000000
C	2.195399000000	-1.471281000000	3.411797000000
H	2.753252000000	-0.969023000000	4.199155000000
H	1.725279000000	-2.341997000000	3.863728000000
C	-0.193149000000	-2.593545000000	2.185893000000
H	-0.780031000000	-2.907130000000	3.053556000000
H	0.738275000000	-3.155753000000	2.205487000000
H	-0.729417000000	-2.926811000000	1.299481000000
C	0.755592000000	3.136770000000	2.005109000000
H	-0.168864000000	3.707159000000	1.952351000000
H	1.311189000000	3.506528000000	2.864343000000
C	-1.633509000000	2.048771000000	0.809579000000
H	-2.210008000000	2.637226000000	1.528187000000
H	-2.365928000000	1.528307000000	0.200701000000
H	-1.109908000000	2.750976000000	0.158167000000
C	2.723010000000	1.381333000000	3.254903000000
H	3.025620000000	2.300785000000	2.758729000000
H	3.558945000000	0.692407000000	3.142842000000
H	2.628942000000	1.605769000000	4.321024000000
N	-0.892033000000	-1.324388000000	-2.374426000000
N	-1.914234000000	-1.091095000000	-0.483869000000

C	1.714914000000	0.561922000000	-2.812481000000
C	1.478673000000	-0.821247000000	-2.779440000000
C	2.380810000000	-1.689416000000	-2.151509000000
C	0.687085000000	1.481989000000	-3.414798000000
H	0.761737000000	2.500834000000	-3.042888000000
H	-0.328614000000	1.155663000000	-3.195752000000
C	-0.728821000000	-1.055232000000	-1.081196000000
H	0.204906000000	-0.836329000000	-0.603960000000
C	0.197167000000	-1.359419000000	-3.366792000000
H	0.308789000000	-2.384502000000	-3.713768000000
H	-0.124380000000	-0.773338000000	-4.225240000000
C	2.082508000000	-3.161025000000	-2.040280000000
H	2.451782000000	-3.587136000000	-1.108675000000
H	2.543427000000	-3.720229000000	-2.859190000000
C	-2.233831000000	-1.544868000000	-2.604934000000
H	-2.614573000000	-1.777288000000	-3.584861000000
C	-2.880080000000	-1.395342000000	-1.415705000000
H	-3.935370000000	-1.439412000000	-1.131243000000
C	-2.148312000000	-0.824586000000	0.949201000000
H	-3.010963000000	-0.155632000000	0.994099000000
H	-2.451939000000	-1.760118000000	1.413060000000
H	5.409631000000	0.152043000000	-0.146455000000
H	0.788830000000	1.527254000000	-4.502642000000
H	1.016279000000	-3.373450000000	-2.064993000000
O	-4.634170000000	0.865996000000	0.300159000000
N	-6.890190000000	0.855891000000	0.417847000000
N	-9.198918000000	0.976689000000	0.594629000000
N	-5.716590000000	-1.063554000000	-0.277212000000
C	-8.106261000000	0.268924000000	0.302346000000
C	-8.125026000000	-1.058339000000	-0.121946000000
C	-5.672456000000	0.218596000000	0.142727000000
C	-6.906935000000	-1.647799000000	-0.392575000000
H	-6.806574000000	1.815444000000	0.721745000000
H	-9.055400000000	-1.592936000000	-0.236586000000
H	-6.893221000000	-2.679162000000	-0.732320000000
H	-10.107262000000	0.554806000000	0.510709000000
H	-9.163870000000	1.935081000000	0.894423000000

PC[1]@Guanine

N	-4.423936000000	-2.433872000000	0.304046000000
N	-3.453323000000	-2.245127000000	2.229530000000
N	0.649798000000	-1.075372000000	-2.403386000000
N	1.621100000000	-0.922021000000	-0.477178000000

C	-3.804779000000	-1.180681000000	-1.723859000000
C	-2.586908000000	-1.590597000000	-2.288400000000
C	-1.729390000000	-0.625519000000	-2.833649000000
C	0.542092000000	-0.229953000000	1.614786000000
C	-4.459758000000	-3.173505000000	2.375701000000
H	-4.659596000000	-3.667129000000	3.312103000000
C	-5.069609000000	-3.292443000000	1.165834000000
H	-5.896934000000	-3.908917000000	0.856028000000
C	-1.893912000000	0.601602000000	2.746326000000
C	-0.349853000000	-1.184628000000	2.129704000000
C	-4.729298000000	-2.212041000000	-1.126891000000
H	-5.772294000000	-1.910771000000	-1.196291000000
H	-4.644957000000	-3.171701000000	-1.632127000000
C	0.218137000000	1.133666000000	1.640318000000
C	-3.454460000000	-1.816529000000	0.971912000000
H	-2.780986000000	-1.090039000000	0.563408000000
C	-2.194723000000	-3.044049000000	-2.279023000000
H	-1.116086000000	-3.182984000000	-2.258066000000
H	-2.571456000000	-3.559430000000	-3.166940000000
C	0.461902000000	-0.804439000000	-1.113874000000
H	-0.472294000000	-0.534659000000	-0.664977000000
C	-0.993286000000	1.539033000000	2.224633000000
C	2.595050000000	-1.277471000000	-1.381954000000
H	3.627524000000	-1.404787000000	-1.061392000000
C	-1.549464000000	-0.758352000000	2.717382000000
C	-0.409267000000	-1.048218000000	-3.429588000000
H	-0.467657000000	-2.038644000000	-3.876262000000
H	-0.089188000000	-0.369097000000	-4.217064000000
C	1.982021000000	-1.376736000000	-2.593304000000
H	2.380271000000	-1.626759000000	-3.561987000000
C	-2.512810000000	-1.776785000000	3.272950000000
H	-1.997799000000	-2.651414000000	3.664229000000
H	-3.107948000000	-1.370242000000	4.087846000000
C	-3.221545000000	1.035962000000	3.309029000000
H	-3.166427000000	1.168183000000	4.393171000000
H	-4.010311000000	0.311286000000	3.111906000000
H	-3.568617000000	1.976915000000	2.888378000000
C	1.825366000000	-0.681470000000	0.965358000000
H	2.632801000000	0.050872000000	1.035388000000
H	2.203652000000	-1.603538000000	1.400106000000
C	1.129513000000	2.160523000000	1.025030000000
H	1.637483000000	2.738499000000	1.801843000000
H	0.575944000000	2.866479000000	0.403101000000

H	1.910164000000	1.725998000000	0.405713000000
C	-0.028373000000	-2.651713000000	2.023550000000
H	0.531179000000	-2.882984000000	1.119178000000
H	-0.918610000000	-3.276581000000	1.997695000000
H	0.576744000000	-2.983702000000	2.871673000000
N	-3.120833000000	3.194698000000	-0.881143000000
N	-2.125981000000	3.374871000000	1.032391000000
C	-2.051067000000	0.738723000000	-2.775275000000
C	-3.273143000000	1.127300000000	-2.208669000000
C	-4.145848000000	0.177254000000	-1.656454000000
C	-1.074556000000	1.763728000000	-3.287173000000
H	-0.042161000000	1.474475000000	-3.096370000000
H	-1.204309000000	2.738191000000	-2.822375000000
C	-2.415089000000	2.542918000000	0.037948000000
H	-2.124247000000	1.512731000000	-0.013840000000
C	-3.629681000000	2.590487000000	-2.132109000000
H	-4.706020000000	2.746570000000	-2.155253000000
H	-3.212413000000	3.154031000000	-2.963730000000
C	-5.415947000000	0.617897000000	-0.978223000000
H	-5.744747000000	-0.079398000000	-0.210910000000
H	-6.233617000000	0.716011000000	-1.697790000000
C	-3.289479000000	4.495303000000	-0.461283000000
H	-3.833199000000	5.223684000000	-1.039448000000
C	-2.663719000000	4.608402000000	0.740934000000
H	-2.562331000000	5.453802000000	1.400771000000
C	-1.349081000000	3.004155000000	2.236953000000
H	-0.462896000000	3.634305000000	2.256752000000
H	-1.948841000000	3.271350000000	3.104436000000
H	-2.582473000000	-3.572178000000	-1.409698000000
H	-1.180299000000	1.904051000000	-4.366496000000
H	-5.306254000000	1.579910000000	-0.480465000000
O	8.971896000000	0.863934000000	0.135620000000
N	6.220487000000	2.291144000000	0.228943000000
N	7.703853000000	-1.047576000000	0.057020000000
N	5.342319000000	-1.108801000000	0.062414000000
N	4.343538000000	1.102397000000	0.180129000000
N	6.565407000000	-3.056968000000	-0.080164000000
C	6.590918000000	0.975383000000	0.162759000000
C	5.417433000000	0.249076000000	0.133643000000
C	7.877750000000	0.357841000000	0.121669000000
C	6.511101000000	-1.710401000000	0.026352000000
C	4.876291000000	2.313785000000	0.237214000000
H	6.850024000000	3.077704000000	0.265998000000

H	8.572639000000	-1.563004000000	0.016257000000
H	4.320953000000	3.237194000000	0.285217000000
H	5.714354000000	-3.566636000000	0.069690000000
H	7.423903000000	-3.557780000000	0.065877000000